Electronic Supplementary Material (ESI) for Dalton Transactions.

Trinuclear coordination assemblies of low-spin dicyano manganese(II) (S = 1/2) and iron(II) (S = 0) phthalocyanines with manganese(II) acetylacetonate and tris(cyclopentadienyl)gadolinium(III) and neodymium(III)

Nikita R. Romanenko,[a] Alexey V. Kuzmin,[b] Maxim V. Mikhailenko,[a] Maxim A. Faraonov,[a] Salavat S. Khasanov,[c] Evgeniya I. Yudanova,[a] Alexander F. Shestakov,[a] Akihiro Otsuka,[c, d] Hideki Yamochi,[c, d] Hiroshi Kitagawa,[c] and Dmitri V. Konarev[a*]

[a]Institute of Problems of Chemical Physics RAS, Chernogolovka, Moscow region, 142432 Russia;

[b]Institute of Solid State Physics RAS, Chernogolovka, Moscow region, 142432 Russia;

[c]Division of Chemistry, Graduate School of Science, Kyoto University, Sakyo-ku, Kyoto 606-8502, Japan;

[d]Research Center for Low Temperature and Materials Sciences, Kyoto University, Sakyo-ku, Kyoto 606-8501, Japan.

Supporting information

EXPERIMENTAL

Materials. Manganese(II) phthalocyanine ($Mn^{II}Pc$, >97%, Strem), iron(II) phthalocyanine ($Fe^{II}Pc$, >90%, Aldrich), iron(II) hexadecachlorophthalocyanine ($Fe^{II}PcCl_{16}$, >98%, Porphychem), tris(cyclopentadienyl)neodymium (Cp_3Nd^{III}, >99%, Strem), tris(cyclopentadienyl)gadolinium (Cp_3Gd^{III}, >99%, Strem), manganese(II) acetylacetonate ($Mn^{II}(acac)_2$, >95%, Strem), potassium cyanide (KCN, >98%, Aldrich). Cryptand[2.2.2] (hereinafter abbreviated as Cryptand) was purchased from Acros. *o*-Dichlorobenzene ($C_6H_4Cl_2$, 99%) was distilled over CaH_2 under reduced pressure in argon atmosphere, and *n*-hexane were distilled over Na/benzophenone in argon atmosphere. Solvents were degassed and stored in an MBraun 150B-G glove box. Complexes **1** - **8** were synthesized and stored in the glove box with controlled atmosphere containing less than 1 ppm of water and oxygen. KBr pellets used for the IR and UV-visible-NIR analyses of **1**-**8** were prepared in the glove box. Magnetic measurements were performed on carefully purified and tested crystals of **1**-**7** sealed in a 2 mm quarz tube under ambient pressure of argon.

General. UV-visible-NIR spectra were measured in KBr pellets on a PerkinElmer Lambda 1050 spectrometer in the 250-2500 nm range. FT-IR spectra were obtained in KBr pellets with a PerkinElmer Spectrum 400 spectrometer (400-7800 cm^{-1}). EPR spectra were recorded for a polycrystalline sample of **1**-**7** from room temperature (295 K) down to liquid helium temperature with a JEOL JES-TE 200 X-band ESR spectrometer equipped with a JEOL ES-CT470 cryostat. A Quantum Design MPMS-XL SQUID magnetometer was used to measure static magnetic susceptibilities of **1**-**4**, **6** and **7** at 1 kOe magnetic field in heating and cooling conditions in the 1.9- 300 K range. A sample holder contribution and core temperature independent diamagnetic susceptibility (χ_d) were subtracted from the experimental data. The χ_d values were estimated by the extrapolation of the data in the high-temperature range by fitting the data with the following expression: $\chi_M = C/(T - \Theta) + \chi_d$, where C is Curie constant and Θ is Weiss temperature. Dependencies of magnetization *vs* magnetic field (up to 5T) were also measured at 1.9-2.0 K for the samples of **2**-**4** cooled in zero field conditions.

Synthesis. Crystals of **1**-**8** were obtained by diffusion technique. The obtained solutions were cooled down to room temperature and filtered into a 1.8 cm diameter, 50 mL glass tube with a ground glass plug, and then 24 mL of *n*-hexane was layered over the solution. Slow mixing of the solutions over 1-1.5 months resulted in precipitation of crystals. The solvent was then decanted from the crystals, and they were washed with *n*-hexane.

Crystals of $\{Cryptand(K^+)\}_2\{Mn^{II}(CN)_2Pc\}^{2-}\cdot C_6H_4Cl_2$ (**1**) and $\{Cryptand(K^+)\}_2\{Fe^{II}(CN)_2Pc\}^{2-}\cdot 0.72C_6H_4Cl_2$ (**5**) were obtained similarly via the interaction of $Mn^{II}Pc$ (24 mg, 0.042 mmol) or $Fe^{II}Pc$ (24 mg, 0.042 mmol) with an excess of KCN (30 mg, 0.46 mmol) and two equivalents of cryptand[2.2.2] (32 mg, 0.084 mmol) in *o*-dichlorobenzene upon stirring the solution at 60^{o}C during one day. Phthalocyanines completely dissolved to form deep violet (for $Mn^{II}Pc$) and deep green (for $Fe^{II}Pc$) solutions. Solutions were cooled down to room temperature and filtered into the glass tubes. After slow mixing with *n*-hexane black crystals were obtained in 62% and 74% yield, respectively. Crystals had the shape of dark black blocks. X-ray diffraction analysis showed that crystals of only one crystal phase formed in each synthesis and all crystals are isostructural (see Table S2) to previously investigated complex $\{Cryptand(K^+)\}_2\{Sn^{II}(NC)_2Pc\}^{2-}\cdot C_6H_4Cl_2$.[1] Elemental analysis confirmed the composition of **1** to be: $C_{76}H_{86}N_{14}O_{12}MnCl_2$, M_r = 1512.66 g mol^{-1}: Calcd. C = 60.34, H = 5.68, N = 12.96, Cl = 4.60%; Found: C = 59.94, H = 5.31, N = 12.88, Cl = 4.52%. The composition of **5** was determined form X-ray diffraction on single crystal. Testing of several crystals from the synthesis showed that all of them belong to one crystal phase (Table S1). It should also be noted that all crystals in the synthesis of **5** had the same shape and color.

Crystals of $\{Cryptand(K^+)\}_2\{Mn^{II}(CN)_2Pc\cdot(Mn^{II}(acac)_2)_2\}^{2-}\cdot 5C_6H_4Cl_2$ (**2**), and $\{Cryptand(K^+)\}_2\{Mn^{II}(CN)_2Pc\cdot(Cp_3Gd^{III})_2\}^{2-}\cdot 4C_6H_4Cl_2$ (**3**) and $\{Cryptand(K^+)\}_2\{Mn^{II}(CN)_2Pc\cdot(Cp_3Nd^{III})_2\}^{2-}\cdot 4C_6H_4Cl_2$ (**4**) were obtained in a similar way. Initially solution of $\{Cryptand(K^+)\}_2\{Mn^{II}(CN)_2Pc\}^{2-}$ salt was obtained via the interaction of $Mn^{II}Pc$ (24 mg, 0.042 mmol) with an excess of KCN (30 mg, 0.46 mmol) and two equivalents of cryptand[2.2.2] (32 mg, 0.084 mmol) in *o*-dichlorobenzene upon stirring the solution at 60^{o}C during one day. Phthalocyanines completely

dissolved to form red-violet solution. They were cooled down to room temperature and filtered into the flask containing 2.26 equivalents of $Mn^{II}(acac)_2$ (24 mg, 0.0948 mmol) for **2** or 2 equivalents of Cp_3Gd^{III} (32 mg, 0.084 mmol) for **3** or 2 equivalents of Cp_3Nd^{III} (32 mg, 0.084 mmol) for **4**. Solutions were stirred additionally during 24 hours at 60°C. Color of the solution changed to dark green. It was cooled down to room temperature and filtered into the glass tube. Slow mixing of the obtained solution with *n*-hexane during 1.5 months produced black blocks in 56, 61 and 48% yield, respectively. Composition of **2** was determined from X-ray diffraction on single crystal. Testing of several crystals from the synthesis showed that all of them belong to one crystal phase (Table S1). It should also be noted that all crystals in the synthesis of **2** had the same shape and color. The same situation was observed for crystals of **3** whose composition was also determined from X-ray diffraction on single crystals (Table S1). Crystals obtained in the synthesis of **4** had the same shape and color and their testing by X-ray diffraction showed that these crystals are isostructural to **3** (Table S2). Therefore, they have the same composition as **3** that was confirmed by elemental analysis: $C_{124}H_{134}Cl_8Nd_2K_2MnN_{14}O_{12}$, M_r = 2713.66 g mol^{-1}: Calcd. C = 54.88, H = 4.94, N = 7.22, Cl = 10.46%; Found: C = 54.22, H = 4.52, N = 7.08, Cl = 10.16%.

Crystals of $\{Cryptand(K^+)\}_2\{Fe^{II}(CN)_2Pc\cdot(Cp_3Nd^{III})_2\}^{2-}\cdot 4C_6H_4Cl_2$ (**6**) were obtained via the $\{Cryptand(K^+)\}_2\{Fe^{II}(CN)_2Pc\}^{2-}$ salt. Solution of this salt was obtained by cyanation of $Fe^{II}Pc$ (24 mg, 0.042 mmol) with an excess of KCN (30 mg, 0.46 mmol) in the presence of two equivalents of cryptand[2.2.2] (32 mg, 0.084 mmol) in *o*-dichlorobenzene upon stirring the solution at 60°C during one day. Phthalocyanines completely dissolved to form deep green solution. It was cooled down to room temperature and filtered into the flask containing 2 equivalents of Cp_3Nd^{III} (32 mg, 0.084 mmol). Solutions were stirred additionally during 24 hours at 60°C. Color of the solution remained unchanged preserving green color. The solution was cooled down to room temperature and filtered into the glass tube. Slow mixing with *n*-hexane during 1.5 months produced black blocks in 42% yield. Crystals obtained in the synthesis of **6** had the same shape and their testing by X-ray diffraction showed that they are isostructural to **3** (Table S2). Therefore, they have the same composition as **3** that was confirmed by elemental analysis: $C_{124}H_{134}Cl_8Nd_2K_2FeN_{14}O_{12}$, M_r = 2714.56 g mol^{-1}: Calcd. C = 54.86, H = 4.94, N =

7.22, Cl = 10.46%; Found: C = 54.47, H = 4.31, N = 7.14, Cl = 10.04%. Small deviation of the content of C, H from the calculated values can be explained by high-air sensitivity of tris(cyclopentadienyl)lanthanides.

Crystals of $\{Cryptand(K^+)\}_2\{Fe^{II}(CN)_2(PcCl_{16})\}^{2-}\cdot 2C_6H_4Cl_2$ (**7**) were obtained by cyanation of Fe^{II}(PcCl16) (47 mg, 0.042 mmol) with an excess of KCN (30 mg, 0.46 mmol) in the presence of two equivalents of cryptand[2.2.2] (32 mg, 0.084 mmol) in *o*-dichlorobenzene upon stirring the solution at 60^{o}C during one day. Phthalocyanine completely dissolved to form deep green solution. It was cooled down to room temperature and filtered into the glass tube. Slow mixing with *n*-hexane during 1.5 months produced black blocks in 54% yield. All crystals obtained in the synthesis of **7** had the same shape and their composition was determined from X-ray diffraction on single crystal. Several crystals tested from the synthesis have the same unit cell parameters (Table S1).

Crystals of $\{Cryptand(K^+)\}_2\{Fe^{II}(CN)_2(PcCl_{16})\cdot(Cp_3Nd^{III})_2\}^{2-}\cdot C_6H_4Cl_2$ (**7**) were obtained via the $\{Cryptand(K^+)\}_2\{Fe^{II}(CN)_2(PcCl_{16})\}^{2-}$ salt. Solution of this salt was obtained by cyanation of $Fe^{II}(PcCl_{16})$ (47 mg, 0.042 mmol) with an excess of KCN (30 mg, 0.46 mmol) in the presence of two equivalents of cryptand[2.2.2] (32 mg, 0.084 mmol) in *o*-dichlorobenzene upon stirring the solution at 60^{o}C during one day. Phthalocyanine completely dissolved to form deep green solution. It was cooled down to room temperature and filtered into the flask containing 2 equivalents of Cp_3Nd^{III} (32 mg, 0.084 mmol). Solutions were stirred additionally during 24 hours at 60^{o}C. Color of the solution remained unchanged. Solution was cooled down to room temperature and filtered into the glass tube. Slow mixing with *n*-hexane during 1.5 months produced black blocks in 71% yield. Crystals obtained in the synthesis of **7** had the same shape and their composition was determined from X-ray diffraction on single crystal. Several crystals tested from the synthesis have the same unit cell parameters (Table S1).

X-ray crystal structure determination

X-ray diffraction data for **1**-**8** are listed in Tables S1 and S2. X-ray diffraction data for **2**, **3**, **5**, **7**, and **8** were collected on an Oxford diffraction "Gemini-R" CCD diffractometer with graphite monochromated MoK_α radiation using an Oxford Instrument Cryojet system. Raw data reduction

to F^2 was carried out using CrysAlisPro, Oxford Diffraction Ltd. The structures were solved by direct method and refined by the full-matrix least-squares method against F^2 using SHELX-2018/3.[2] Non-hydrogen atoms were refined anisotropically. Positions of hydrogen atoms were included into refinement in a riding model. Crystal structure of **2** contains only half independent $\{Mn^{II}(CN)_2Pc\cdot(Mn^{II}(acac)_2)_2\}^{2-}$ dianion, one independent {Cryptand[2.2.2](K^+)} cation and 2.5 independent $C_6H_4Cl_2$ molecules. Among solvent molecules one molecule is fully ordered, another molecule is disordered between two orientations with 0.771(2)/0.229(2) occupancies and a third molecule is positioned in the inversion center and has only 0.5 occupancy. Crystal structure of **3** contains only half independent $\{Mn^{II}(CN)_2Pc\cdot(Cp_3Gd^{III})_2\}^{2-}$ dianion, one independent {Cryptand[2.2.2](K^+)} cation and two independent $C_6H_4Cl_2$ molecules. Among solvent molecules one molecule is fully ordered, whereas another molecule is disordered between two orientations with 0.6507(18)/0.3493(18) occupancies. Crystal structure of complex 5 is isostructural to previously described complex $\{Cryptand(K^+)\}_2\{Sn^{II}(NC)_2Pc\}^{2-}\cdot C_6H_4Cl_2$[1]. As a result, complex 2 also contains position occupied by strongly disordered $C_6H_4Cl_2$ molecules which were squeezed by standard Olex2 routine. According to the estimated electron density the content of $C_6H_4Cl_2$ is slightly smaller than 1 (0.72). The reason of that can be the loose of solvent during the storage of crystals. Crystal structure of **7** contains only half independent $(Cryptand[2.2.2](K^+)\}_2\{Fe^{II}(CN)_2PcCl_{16}\}^{2-}$ unit and one independent $C_6H_4Cl_2$ molecule which is disordered between two orientations with 0.6065(17)/0.3935(17) occupancies. Crystal structure of **8** contains one independent $\{Fe^{II}(CN)_2(PcCl_{16})\cdot(Cp_3Nd^{III})_2\}^{2-}$ dianion, two independent ordered {Cryptand[2.2.2](K^+)} cations and one independent $C_6H_4Cl_2$ molecule which is disordered between two orientations with 0.507(4)/0.493(4) occupancies. To keep anisotropic thermal parameters of the disordered fragments, the displacement components were restrained using SHELXL instructions of ISOR, SIMU and DELU. That resulted in the use of some amount of restraints for the refinement of crystal structures of **2**, **3**, **5**, **7** and **8**: 18, 54, 288, 276 and 832, respectively.

Table S1. Crystallographic data and some details of the data collection and refinement for **2, 3**, **7** and **8**.

Compound	**2**	**3**	**5**	**7**	**8**
Empirical formula	$C_{120}H_{136}Cl_{10}K_2Mn_3N_{14}O_{20}$	$C_{124}H_{134}Cl_8Gd2K_2MnN_{14}O_{12}$	$C_{74.3}Cl_{1.4}Fe\ H_{90.9}K_2N_{14}O_{12}$	$C_{82}H_{80}Cl_{20}FeK_2N_{14}O_{12}$	$C_{106}H_{106}Cl_{18}FeK_2N_{14}Nd_2O_{12}$
M_r [g·mol^{-1}]	2691.94	2743.68	1563.13	2296.65	2828.67
Crystal color and shape,	Dark black block	Dark black block	Dark black block	Dark black block	Dark black block
Crystal system	Monoclinic	Triclinic	Triclinic	Monoclinic	Triclinic
Space group	$P\ 2_1/n$	$P\ \bar{1}$	$P\ \bar{1}$	$P\ 2_1/n$	$P\ \bar{1}$
a, Å	16.7101(5)	13.9492(3)	12.7789(6)	13.1832(1)	16.2343(3)
b, Å	18.1789(4)	14.2598(2)	13.5071(8)	19.5040(2	19.4760(5)
c, Å	22.3440(7)	17.5018(3)	13.6608(8)	19.3262(2)	20.9495(6)
α, °	90	73.112(2)	111.912(6)	90	108.677(3)
β, °	107.465(3)	78.193(2)	111.362(5)	102.044(1)	95.219(2)
γ, °	90	67.321(2)	94.970(4)	90	110.988(2)
V, Å^3	6474.6(3)	3056.67(11)	1968.5(2)	4859.87(8)	5698.1(3)
Z	2	1	1	2	2
ρ_{calc} [g/cm^3]	1.381	1.491	1.319	1.569	1.649
μ [mm^{-1}]	0.628	1.483	0.399	0.856	1.585
F(000)	2794	1399	823	2340	1649
T [K]	109(2)	106(2)	150(2)	111(2)	101(2)
2Θ, °	52.000	52.000	59.068	59.380	52.000
Reflns measured	74099	36115	36467	52980	60835
Unique reflns	12731	12027	9677	12195	22320
Params/Restraints	762/18	791/54	448/288	665/276	1467/832
Reflns [$F_o>2\sigma(F_o)$]	9592	11622	3132	10260	16309
R_1 [$F_o>2\sigma(F_o)$]/wR_2(all)	0.0594/0.1461	0.0259/0.0647	0.1261/0.4374	0.0314/0.0784	0.0775/0.1275
G.O.F	1.043	1.043	1.065	1.016	1.152
CCDC number	2117285	2117286	2161670	2117284	2117330

Table S2. Unit cell parameters determined for the structures of reference salt and compounds **1**, **4** and **6**.

Compound	$\{Cryptand(K^+)\}_2\{Sn^{II}(NC)_2Pc\}^{2-}\cdot C_6H_4Cl_2$ [1]	**1**	**4**	**6**
Crystal system	Triclinic	Triclinic	Triclinic	Triclinic
Space group	$P\ \bar{1}$	$P\ \bar{1}$	$P\ \bar{1}$	$P\ \bar{1}$
a, Å	12.7619(3)	12.80(2)	14.10(2)	13.945(8)
b, Å	13.3263(3)	13.43(2)	14.50(2)	14.574(8)
c, Å	14.0032(3)	14.11(2)	17.83(2)	17.793(9)
α, °	63.247(2)	62.41(8)	74.27(12)	74.64(5)
β, °	74.649(2)	74.42(8)	78.20(11)	77.99(5)
γ, °	67.758(2)	67.78(8)	67.18(14)	67.38(5)
V, Å^3	1955.49(9)	1978(8)	3213(8)	3196(3)
T, K	120	250	250	250

Table S3. IR spectra of starting compounds and complexes **1-4**.

Components	Cp_3Nd^{III}	$Mn^{II}(acac)_2$	Cryptand [2.2.2]	$\{Cryptand(K)\}_2\{Mn^{II}(CN)_2Pc\}\cdot C_6H_4Cl_2$ (**1**)	$\{Cryptand(K)\}_2\cdot\{[Mn^{II}(acac)_2]_2Mn^{II}(CN)_2Pc\}\cdot 5C_6H_4Cl_2$ (**2**)	$\{Cryptand(K)\}_2\cdot\{(Cp_3Gd^{III})_2Mn^{II}(CN)_2Pc\}\cdot 4C_6H_4Cl_2$ (**3**)	$\{Cryptand(K)\}_2\{(Cp_3Nd^{III})_2Mn^{II}(CN)_2Pc\}\cdot 4C_6H_4Cl_2$ (**4**)
$Mn^{II}(CN)_2(Pc^{2-})$				435w 510w 570w 727s* 751s* 765m 821w 828w 832w 932m* 951s* 1002w 1058m 1078s* 1117vs* 1164s 1262m 1290m 1330m* 1419m 1466w* 1478m 1496s* 1582w 2094m (CN) 3054w	434w* 511w 570w 728s* 751s* 767m* 820w 833w 934m* 950s* 1003w 1059m 1080s* 1116vs* 1163m 1257m 1288m* 1297m 1331w* 1419s 1457m* 1478m 1498s* 1594s* 2098m (CN) 3052w	433w 510w 570w 729s* 751s* 769m 820w 831w 933m 949s 1004w 1059m 1081s 1116vs* 1164m 1259m 1288m*1296m* 1330m* 1418m 1457w* 1478m 1498s* 1584w 2097m (CN) 3054w	432w 511w 571w 729s* 752s* 767m 820w 831w 931m 950s* - - 1080s* 1118vs* 1163m 1259m 1288m* 1297m* 1331w* 1420m 1457m* 1478m 1499s* 1584w 2098m (CN)
$Cryptand(K^+)$			476w 528w 581w 735m 922m 948w 982m 1038w 1071m 1100s 1127s 1213w - 1290m 1329m 1360s 1446m 1462m 1490w 2790w 2877w 2943w	476w 523w - 727s* 920w 951s* - 1034w* 1078s* 1102vs 1117vs* 1240w 1290w 1330m* 1355m* 1444w 1466w* 1496s* 2810w 2873w 2954w	476w 524w - 728s* 920w 950s* - 1032w* 1080s* 1105vs 1116vs 1240w 1288m* 1297m* 1331w* 1354m 1360m - 1457m* 1498s* 2815w 2883w 2959w	- 522w - 729s* 916w 949s - 1032w* 1081s* 1104vs 1116vs* 1240w 1288m* 1296m* 1330m* 1354s 1360s 1445w* 1457w* 1498s* 2812w 2883m 2957w	- 524w - 729s* - 950s* - 1033m* 1080s* 1104vs 1118vs* 1240w 1288m* 1297m* 1331m* 1354m 1361m 1444w* 1457m* 1499s* 2812w 2883m 2957w
Metal fragment	753s 882w 1005s 1070w 1123w 1264w 1340w 1440w 3085w	406w 446m 544m 646w 769w 918w 937w 1013w 1192w 1252s 1362s 1506s 1601s			$Mn^{II}(acac)_2$ 408w 434w* 544w - 767m* 920w 934m* 1015w 1189w 1257m* 1360m 1512s 1594s*	Cp_3Gd^{III} 751s* 884w 1013m 1081s* 1131w 1260m 1330m* 1445w* 3080w	Cp_3Nd^{III} 752s* 882w 1013m 1080s* 1133w 1258m 1331w* 1444w* 3080w
$C_6H_4Cl_2$				659w 751s* 1034w* 1455m	658w 751s* 1032w* 1457m*	664w 751s* 1032w* 1457w*	658w 751s* 1033m* 1457m*

*- bands are coincided; w – weak intensity, m –middle intensity, s – strong intensity; vs- very strong

Table S4. IR spectra of obtained complexes **5-8**.

Components	$\{Cryptand(K)\}_2\{Fe^{II}(CN)_2Pc\}\cdot C_6H_4Cl_2$ (**5**)	$\{Cryptand(K)\}_2\{(Cp_3Nd^{III})_2Fe^{II}(CN)_2Pc\}\cdot 4C_6H_4Cl_2$ (**6**)	$\{Cryptand(K)\}_2\{Fe^{II}(CN)_2(PcCl_{16})\}\cdot 2C_6H_4Cl_2$ (**7**)	$\{Cryptand(K)\}_2\{(Cp_3Nd^{III})_2Fe^{II}(CN)_2(PcCl_{16})\}\cdot C_6H_4Cl_2$ (**8**)
$Fe^{II}(CN)_2(Pc^{2-}$ or $PcCl_{16}^{2-})$	432w	433w	435w	437w
	572w	571w	505s	509m
	734s*	734s*	605w	607w
	753s*	752s*	755s	752s* 756s
	773m	775m	760s	760s 764s
	820w	820w	772s	773s
	831w	830w	820w	825w
	932m	932m	830w	-
	948m*	950m*	932m	931m
	-	-	950m*	948s*
	1004w	-	1079m	1079m*
	1079m*	1078m	1160s 1167s	1158s
	1164m	1164m	1218w	1210w
	1260m	1260m	1260m 1274m	1260m* 1272m
	1290m*	1287m* 1296m*	1297s* 1308s 1316s*	1299s* 1310s 1319w*
	1354s*	1353m*	1350m 1358m	1353m* 1360m
	1360m	1354s* 1361s*	1390m	1389m
	1421s	1421m	1455m*	1454m*
	1457m*	1457w*	1474m	1477m
	1477m	1476w	1507s	1507s
	1510s	1511s	1540s	1539m
	1587w	1587w	1602w	1599w
	2093m (CN)	2091m (CN)	2099m (CN)	2097 s (CN)
	3053w	3052w	2105w (CN)	2114w (CN)
			3059w	3058 w
$Cryptand(K^+)$	-	-	-	-
	523w	524w	-	-
	734s*	734s*	-	-
	916w	915w	915w*	-
	948m	950m*	950m*	948s*
	-	-	-	-
	1033w*	1033w*	1033w*	1032*
	1079m*	1078m*	1078s*	1078m*
	1101vs	1101s	-	-
	1117vs	1118s	1110vs*	1105vs
	1239w	1240w	-	-
	1290m*	1287m* 1296m	1297s*	1299s*
	1332m*	1332w*	1316m*	1319w*
	1354s*	1354s* 1361s*	1350m 1358m	1353s
	-	1445w*	1444w	1444w*
	1457m*	1457w*	1466w*	-
	2811w	2812w	2808w	2814w
	2885w	2881w	2878w	2881m
	2955w	2960w	2957w	2955w
Metal fragment		Cp_3Nd^{III}		Cp_3Nd^{III}
		752s*		752s*
		891w		881w
		1012w		1014m
\		1078m		1079m*
		-		1132m
		1259w		1260m*
		1333w*		-
		1445w*		1444w*
		3077w		3088w
$C_6H_4Cl_2$	658w	664w	658w	656w
	753s*	752s*	752s*	752s*
	1033w*	1033w	1033w*	1032w*
	1457m*	1457w*	1455m*	1454m*

* - bands are coincided; w – weak intensity, m –middle intensity, s – strong intensity

IR spectra of starting compounds and obtained complexes.

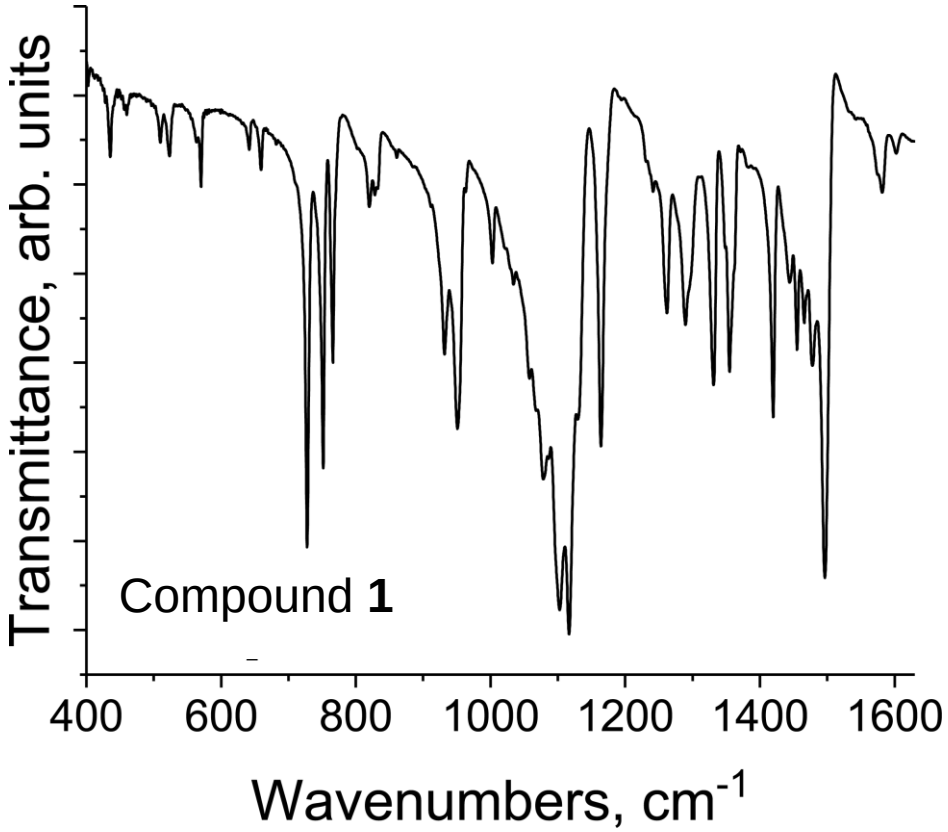

Figure S1. IR spectrum of {Cryptand(K)}$_2${$Mn^{II}(CN)_2Pc$}·$C_6H_4Cl_2$ (**1**) in KBr pellet prepared in anaerobic conditions.

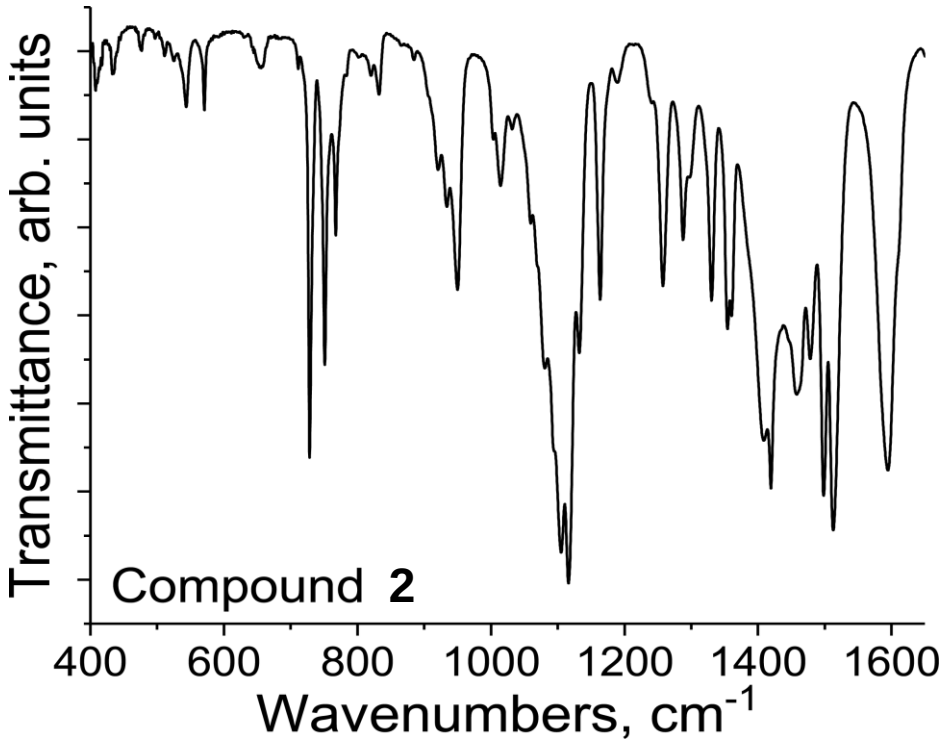

Figure S2. IR spectrum of {Cryptand(K)}$_2$·{Mn^{II}(CN)$_2$Pc·[Mn^{II}(acac)$_2$]$_2$}·5C$_6$H$_4$Cl$_2$ (**2**) in KBr pellet prepared in anaerobic conditions.

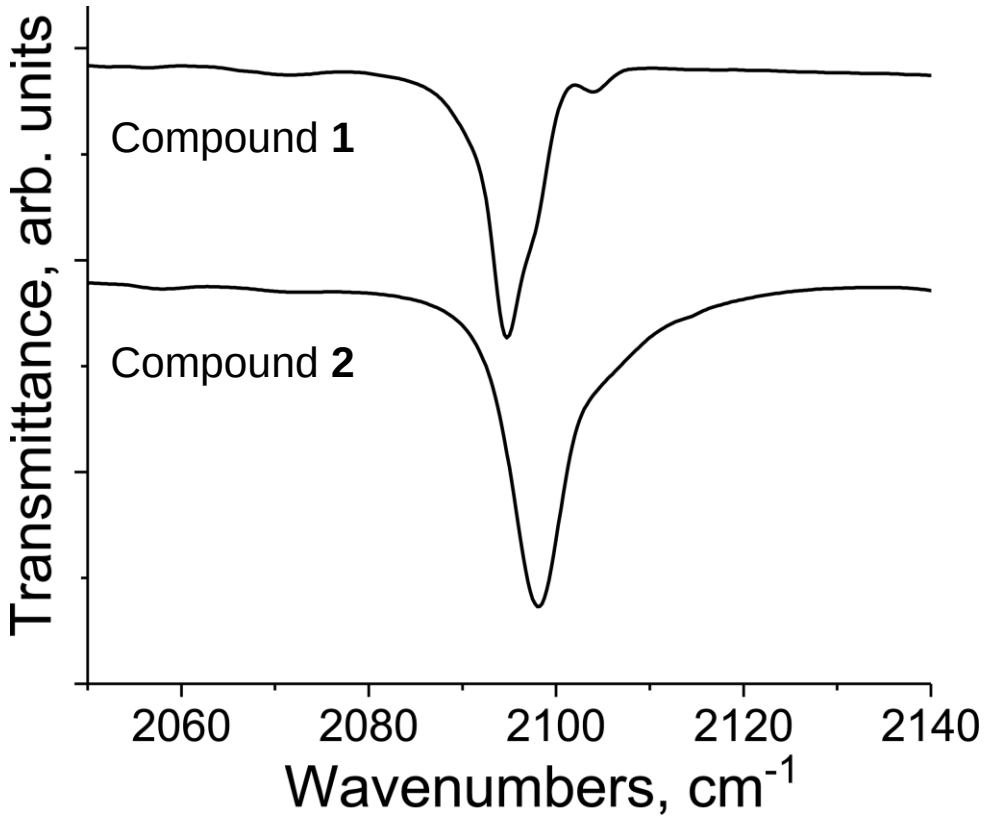

Figure S3. IR spectra of compounds {Cryptand(K)}$_2${Mn^{II}(CN)$_2$Pc}·C$_6$H$_4$Cl$_2$ (**1**) and {Cryptand(K)}$_2$·{Mn^{II}(CN)$_2$Pc·[Mn^{II}(acac)$_2$]$_2$}·5C$_6$H$_4$Cl$_2$ (**2**) in the field of the C≡N vibrations (2050-2140 cm^{-1}·). Spectra are measured in KBr pellets prepared in anaerobic conditions.

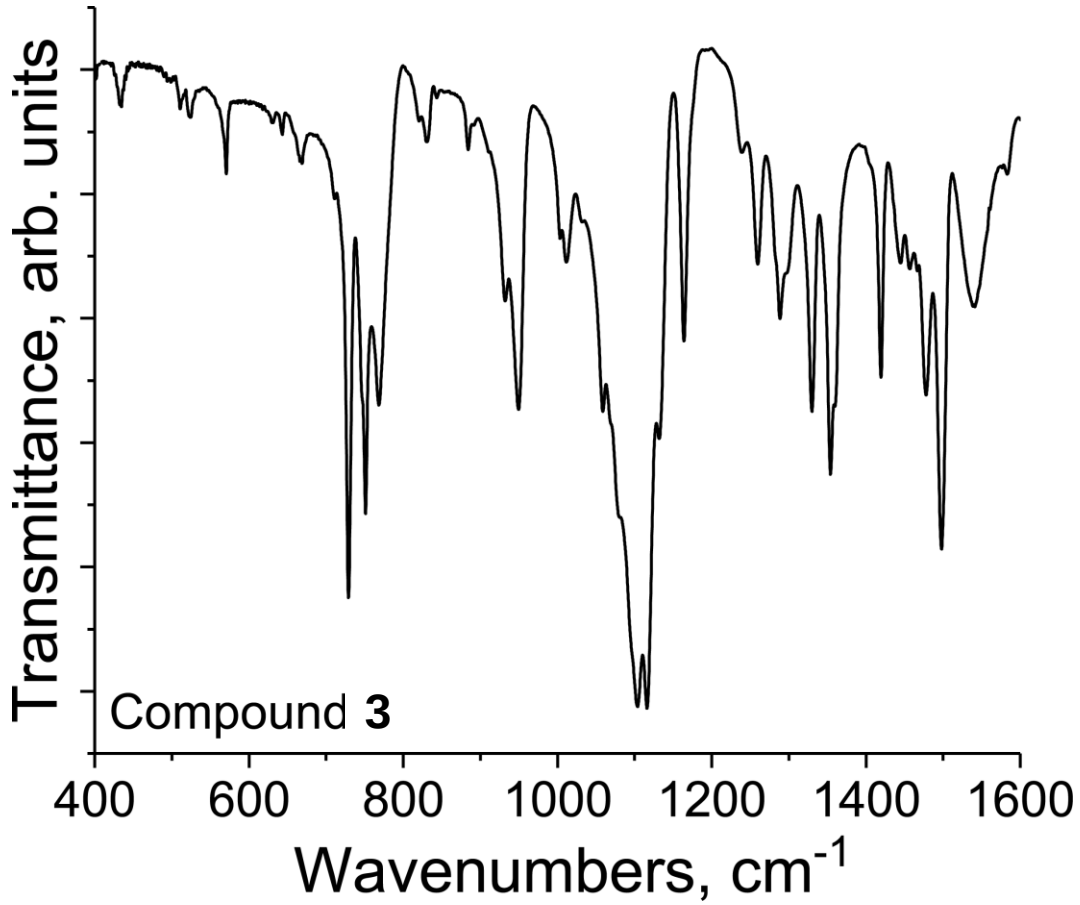

Figure S4. IR spectrum of $\{Cryptand(K)\}_2 \cdot \{(Cp_3Gd^{III})_2Mn^{II}(CN)_2Pc\} \cdot 4C_6H_4Cl_2$ (**3**) in KBr pellet prepared in anaerobic conditions.

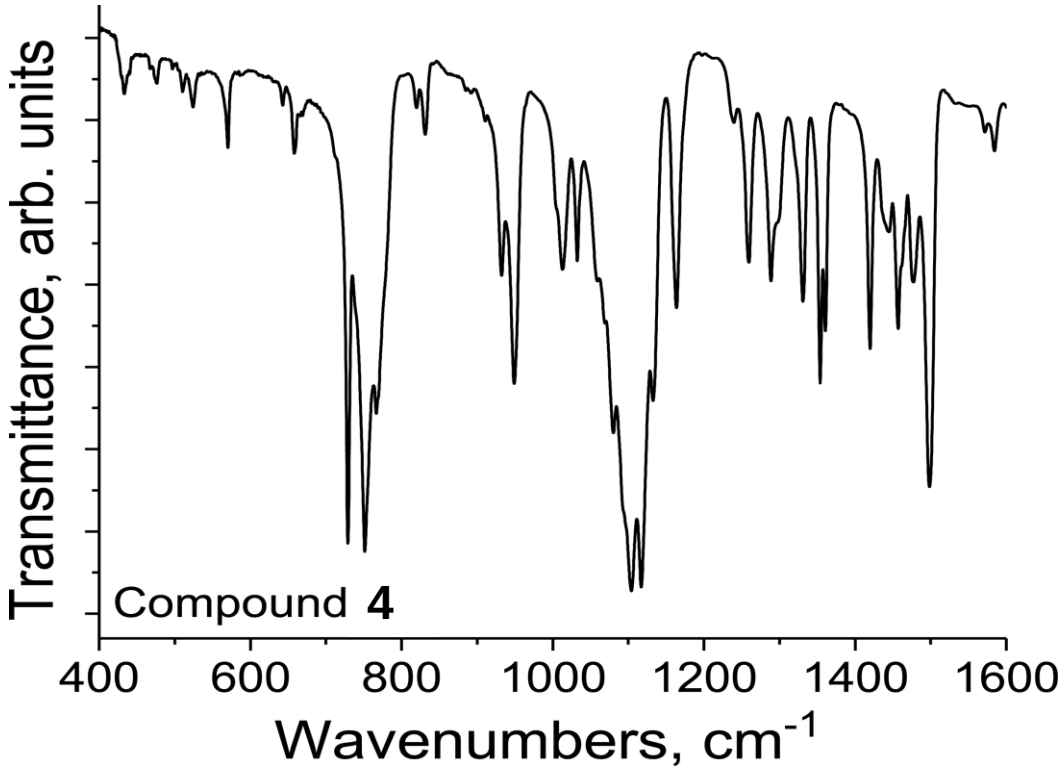

Figure S5. IR spectrum of {Cryptand(K)}$_2$·{(Cp$_3$Nd^{III})$_2$Mn^{II}(CN)$_2$Pc}·4C$_6$H$_4$Cl$_2$ (**4**) in KBr pellet prepared in anaerobic conditions.

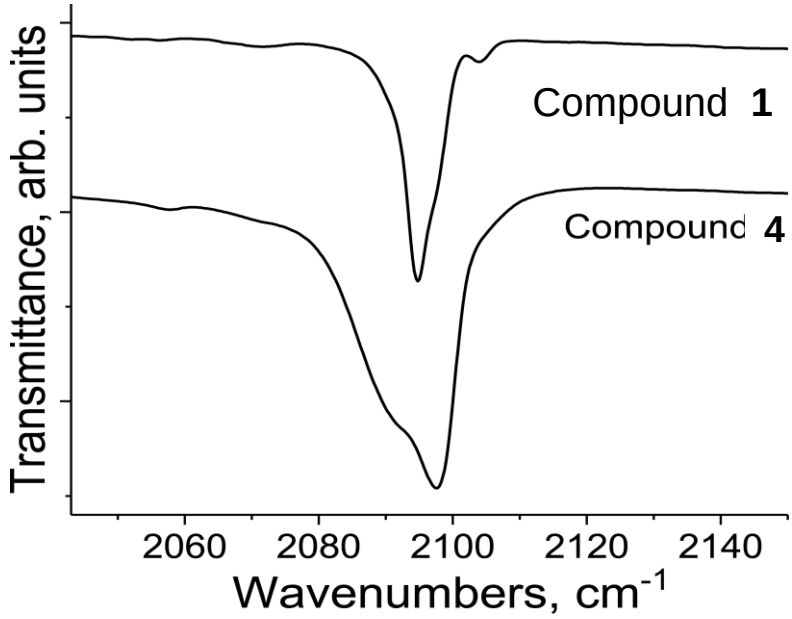

Figure S6. IR spectra of compounds {Cryptand(K)}$_2${Mn^{II}(CN)$_2$Pc}·C$_6$H$_4$Cl$_2$ (**1**) and {Cryptand(K)}$_2${(Cp$_3$Nd^{III})$_2$Mn^{II}(CN)$_2$Pc}·4C$_6$H$_4$Cl$_2$ (**4**) in the field of the C≡N vibrations (2040-2150 cm^{-1}). Spectra are measured in KBr pellets prepared in anaerobic conditions.

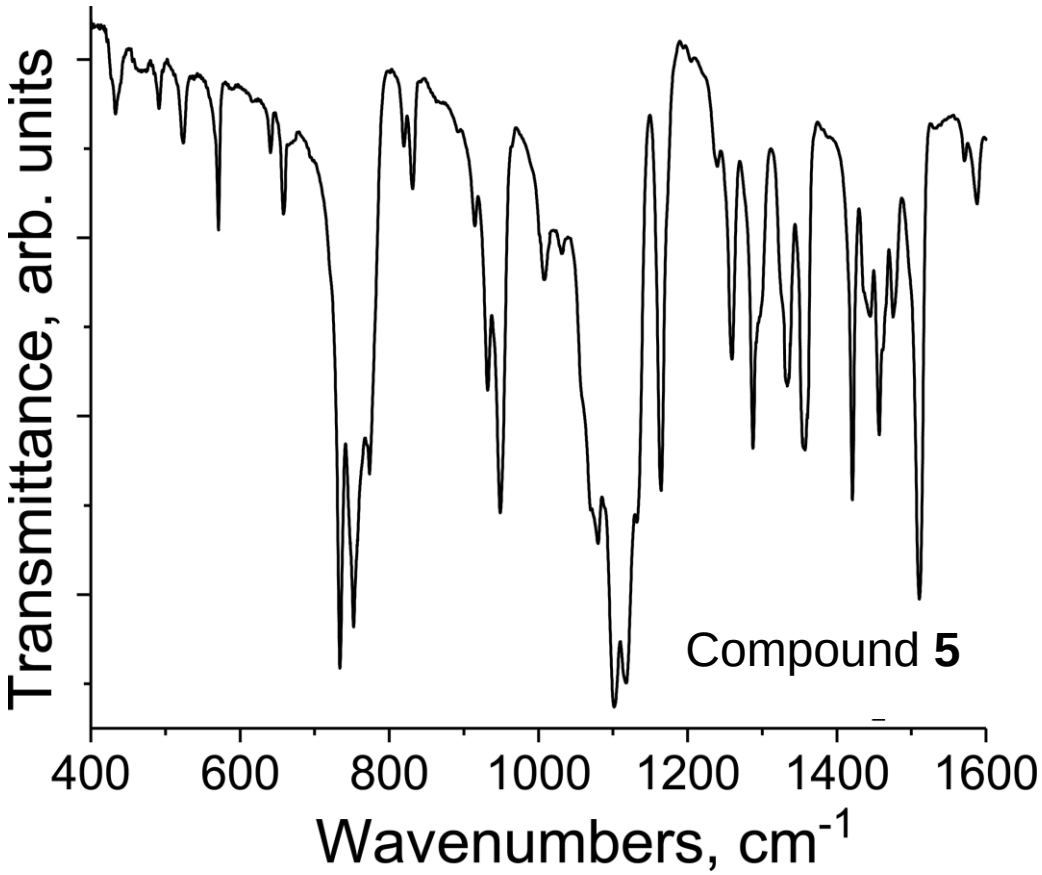

Figure S7. IR spectrum of compound $\{Cryptand(K)\}_2\{Fe^{II}(CN)_2Pc\}\cdot C_6H_4Cl_2$ (**5**) in KBr pellet prepared in anaerobic conditions.

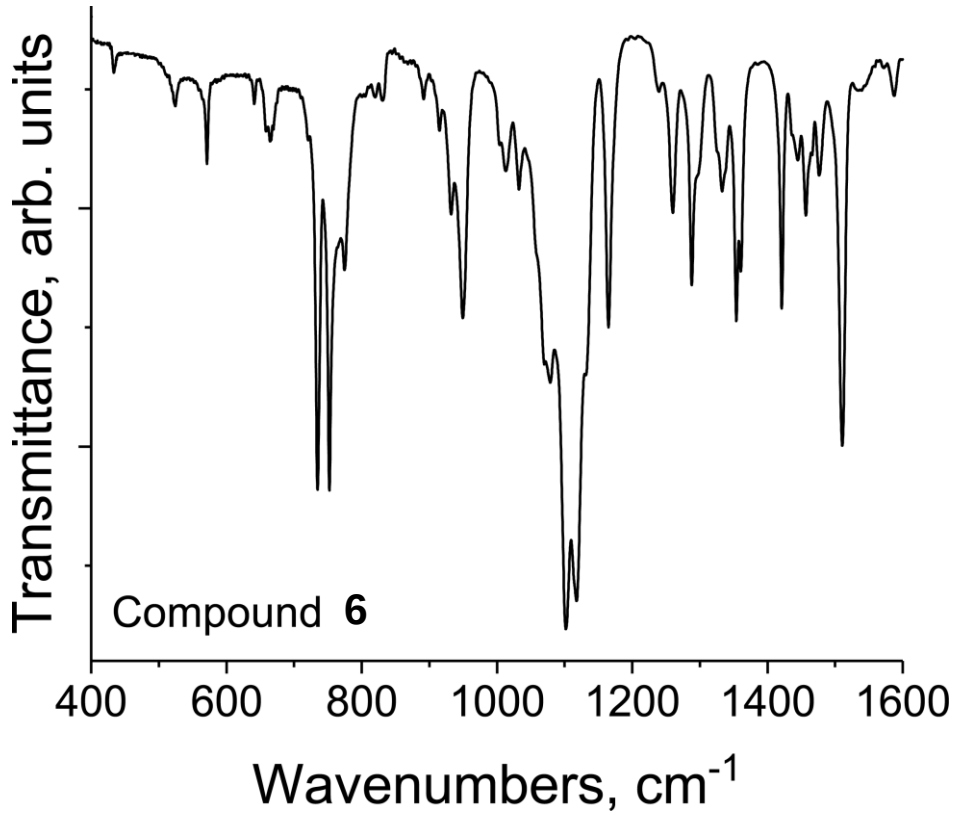

Figure S8. IR spectrum of $\{Cryptand(K)\}_2\{(Cp_3Nd^{III})_2Fe^{II}(CN)_2Pc\}\cdot 4C_6H_4Cl_2$ (**6**) in KBr pellet prepared in anaerobic conditions.

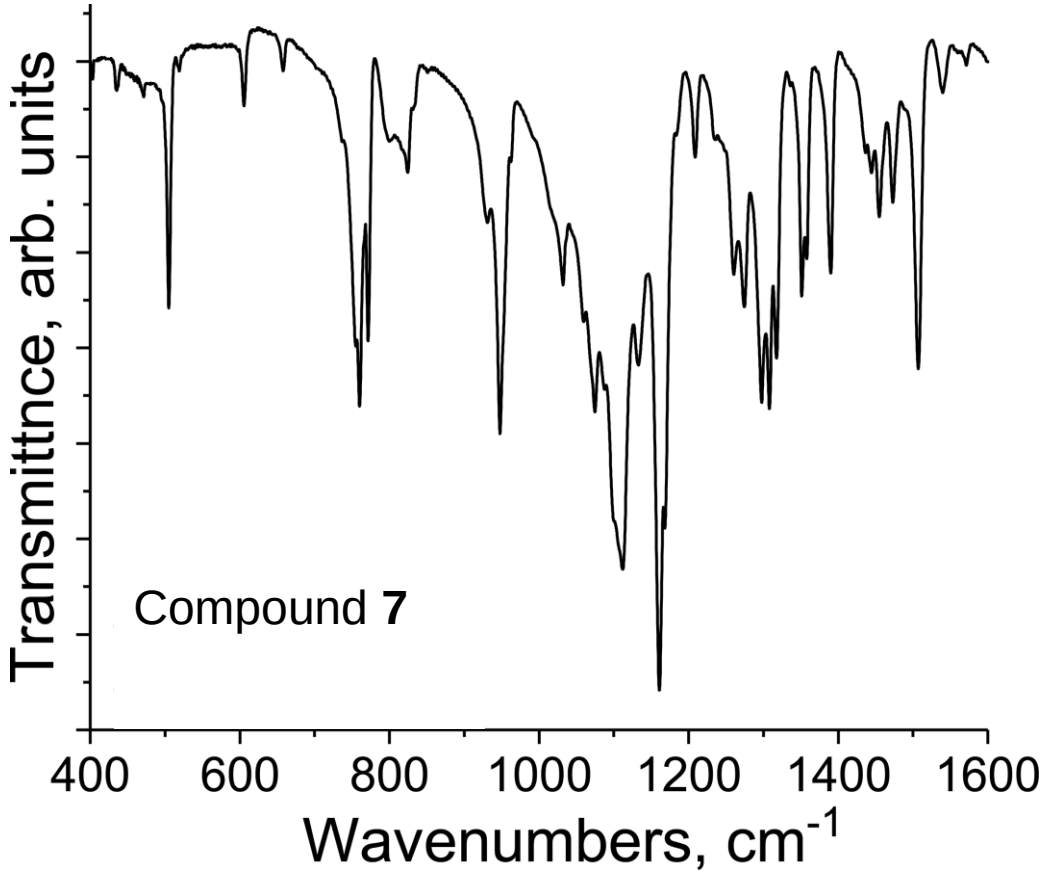

Figure S9. IR spectrum of compound $\{Cryptand(K)\}_2\{Fe^{II}(CN)_2(PcCl_{16})\}\cdot 2C_6H_4Cl_2$ (**7**) in KBr pellet prepared in anaerobic conditions.

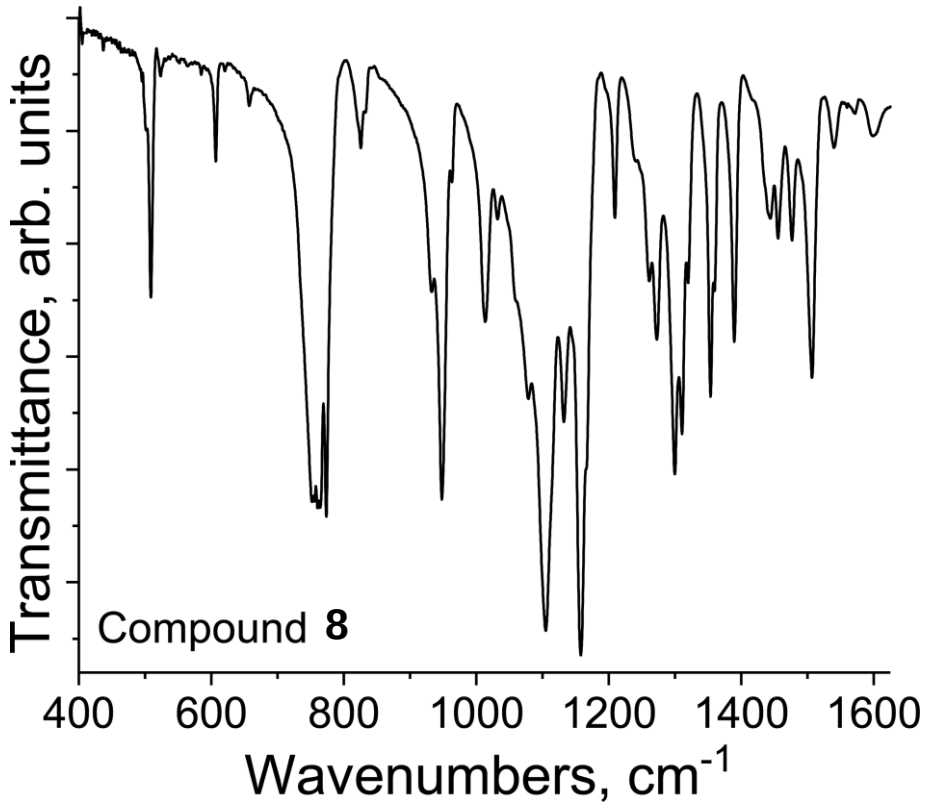

Figure S10. IR spectrum of compound $\{Cryptand(K)\}_2\{(Cp_3Nd^{III})_2Fe^{II}(CN)_2(PcCl_{16})\}\cdot C_6H_4Cl_2$ (**8**) in KBr pellet prepared in anaerobic conditions.

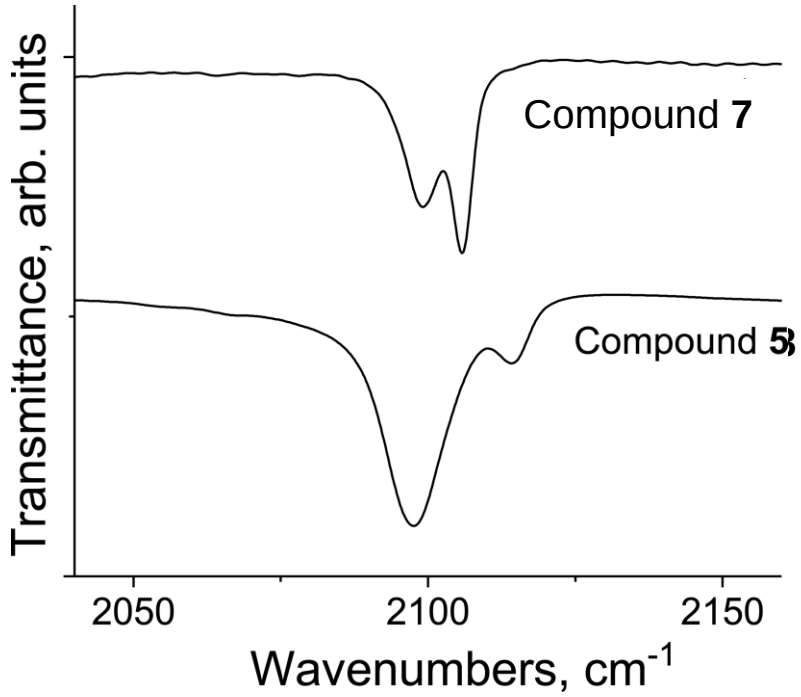

Figure S11. IR spectra of compounds $\{Cryptand(K)\}_2\{Fe^{II}(CN)_2(PcCl_{16})\}\cdot 2C_6H_4Cl_2$ (**7**) and $\{Cryptand(K)\}_2\{(Cp_3Nd^{III})_2Fe^{II}(CN)_2(PcCl_{16})\}\cdot C_6H_4Cl_2$ (**8**) in the field of the C≡N vibrations (2040-2160 cm^{-1}). Spectra are measured in KBr pellets prepared in anaerobic conditions.

Table S5. Optical spectra of reference and obtained complexes.

N	and unit	Soret band	Bands at 380-570 nm	Q-band
	$Mn^{II}Pc$	349	-	690, 736
	$\{Cryptand(K^+)\}^+)\}\{Fe^I(Pc^{2-})\}^-\cdot C_6H_4Cl_2$ [3]	316	406, 442, 477, 526, 557	688 (max), 822
1	$\{Mn^{II}(CN)_2Pc\}^{2-}$	319, 329	385, 400 , 451, 495, 521 (sh), 568	598, 660 (max), 684(sh), 805
2	$\{Mn^{II}(CN)_2Pc\cdot(Mn^{II}(acac)_2)_2\}^{2-}$	286, 300, 317	383, 443, 473, 531	598, 668 (max), 684 (sh), 815
3	$\{Mn^{II}(CN)_2Pc\cdot(Cp_3Gd^{III})_2\}^{2-}$	325,	383, 443(sh), 473, 532	598, 660 (max), 688, 817
4	$\{Mn^{II}(CN)_2Pc\cdot(Cp_3Nd^{III})_2\}^{2-}$	334,	383, 447(sh), 482, 544	598, 667, 687 (max), 811
	$Fe^{II}Pc$	326	-	670
5	$\{Fe^{II}(CN)_2Pc\}^{2-}$	311, 382	-	601, 669(max)
6	$\{Fe^{II}(CN)_2Pc\cdot(Cp_3Nd^{III})_2\}^{2-}$	312, 388	-	607, 672(max)
7	$\{Fe^{II}(CN)_2(PcCl_{16})\}^{2-}$	336	427, 486	624, 691(max)
8	$\{Fe^{II}(CN)_2(PcCl_{16})\cdot(Cp_3Nd^{III})_2\}^{2-}$	342	407, 458	622, 687(max)

UV-visible-NIR spectra

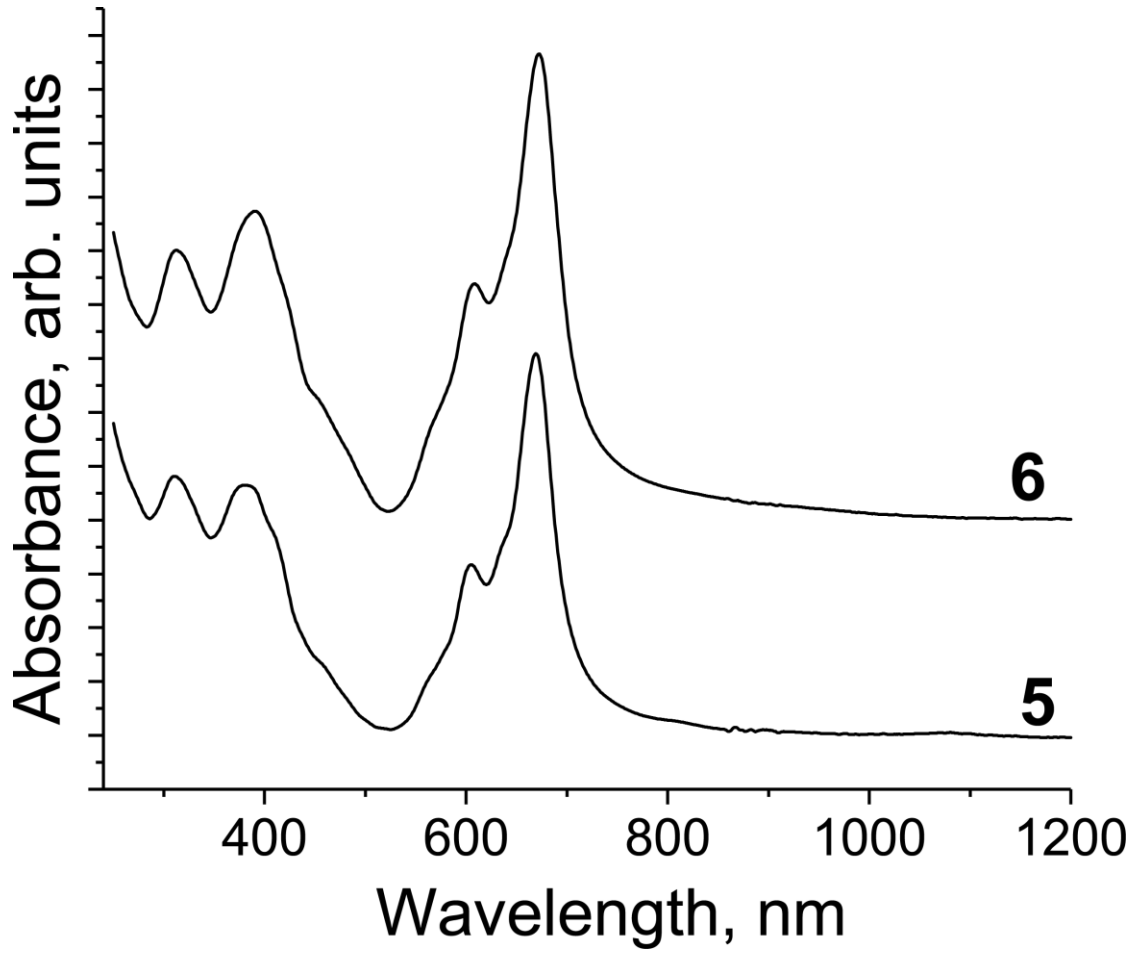

Figure S12. UV-visible-NIR spectra of compound **5** containing $\{Fe^{II}(CN)_2Pc\}^{2-}$ dianions and compound **6** with the $\{Fe^{II}(CN)_2Pc\cdot(Cp_3Nd^{III})_2\}^{2-}$ dianions.

Crystal structures of the obtained complexes.

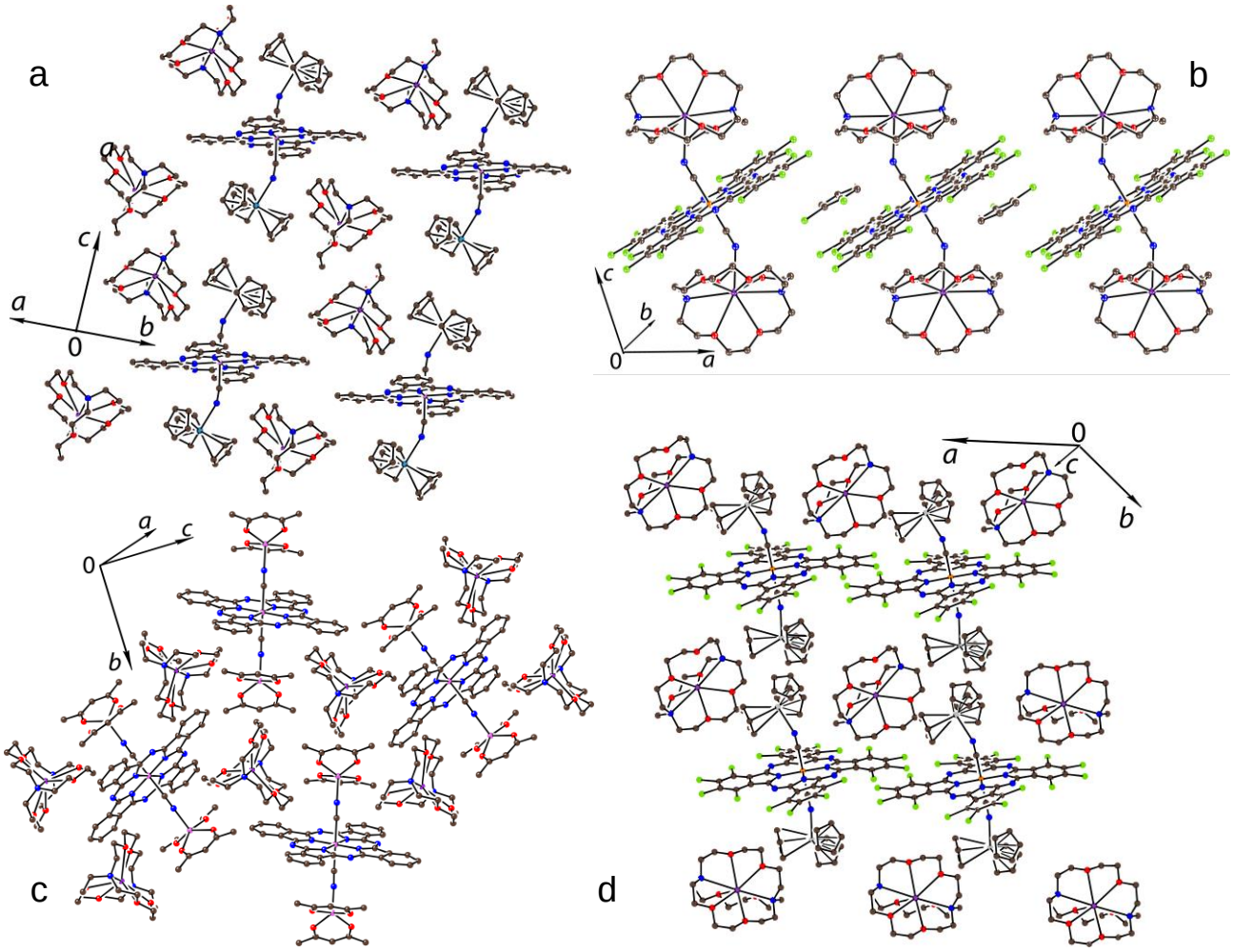

Figure S13. Crystal structures of: (a) $\{Cryptand(K^+)\}_2\{Mn^{II}(CN)_2Pc\cdot(Cp_3Gd^{III})_2\}^{2-}\cdot 5C_6H_4Cl_2$ (**3**); (b) $\{Cryptand(K^+)\}_2\{Fe^{II}(CN)_2PcCl_{16}\}^{2-}\cdot 2C_6H_4Cl_2$ (**7**); (c) $\{Cryptand(K^+)\}_2\{Mn^{II}(CN)_2Pc\cdot(Mn^{II}(acac)_2)_2\}^{2-}\cdot 5C_6H_4Cl_2$ (**2**); and (d) $\{Cryptand(K^+)\}_2\{Fe^{II}(CN)_2(PcCl_{16})\cdot(Cp_3Nd^{III})_2\}^{2-}\cdot C_6H_4Cl_2$ (**8**). Solvent $C_6H_4Cl_2$ molecules are not shown for clarity excluding compound **7**.

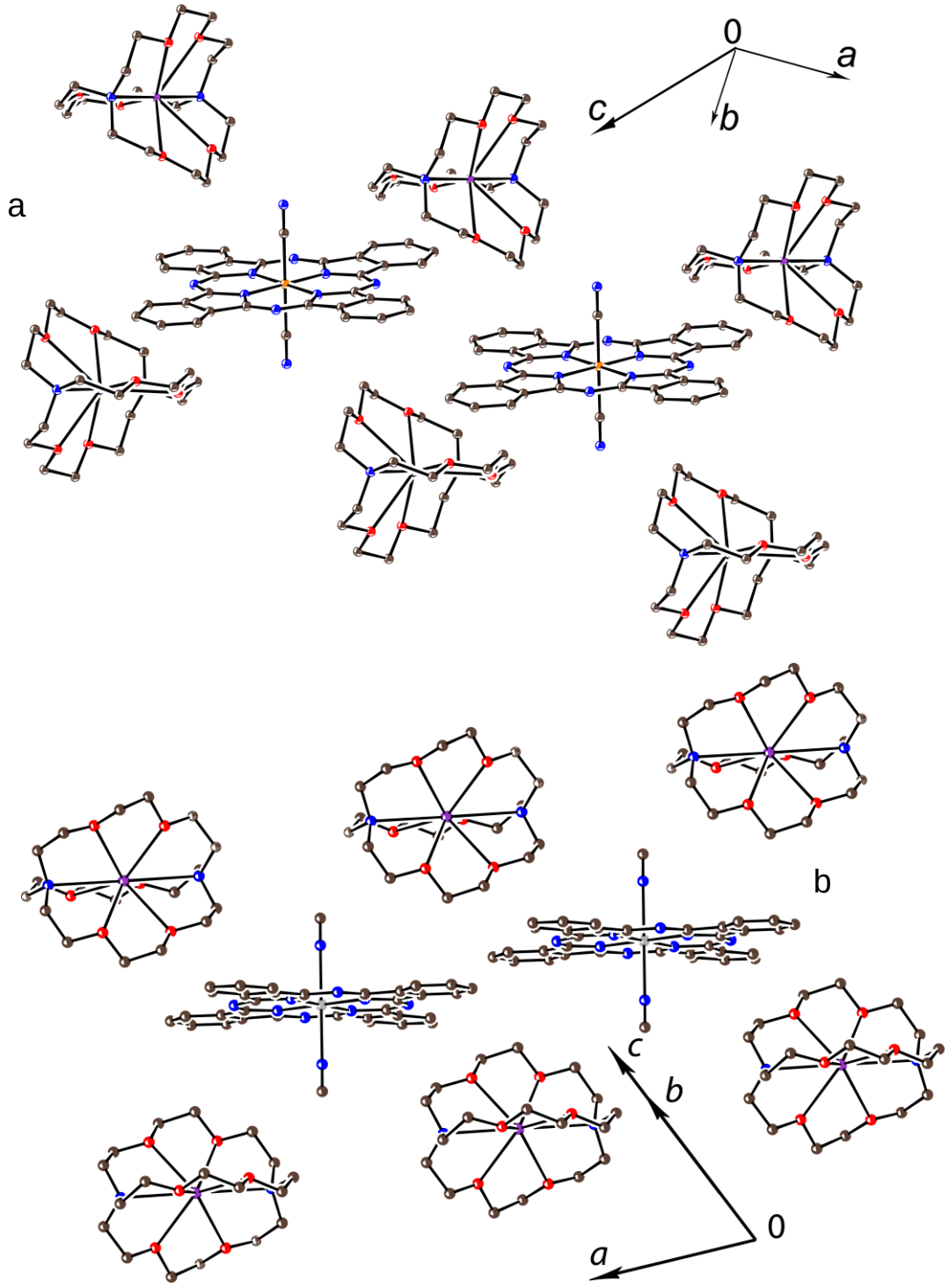

Figure S14. Crystal structures of isostructural salts $\{Cryptand(K^+)\}_2\ \{Fe^{II}(CN)_2(Pc^{2-})\}^{2-}\cdot 0.72C_6H_4Cl_2$ (**5**) (a) and previously published salt $\{Cryptand(K^+)\}_2\{Sn^{IV}(NC)_2(Pc^{4-})\}^{2-}\cdot C_6H_4Cl_2$ [1]. Compound $\{Cryptand(K^+)\}_2\{Mn^{II}(CN)_2(Pc^{2-})\}^{2-}\cdot C_6H_4Cl_2$ (**1**) studied in this work is isostructural to these salts.

Table S6. Data of magnetic measurements for **1-7.**

Compound, units and their spin state	SQUID data	EPR data, g-factor (linewidth, mT)
1, $\{Mn^{II}(CN)_2Pc\}^{2-}$ (S =1/2)	$\chi_M T$ = 0.41 emu·K/mol at 300 K, Θ = -5 K (10-300 K)	293 K, g_1 = 2.1116 (8.12), g_2 = 2.0746 (10.67), g_3 = 1.9895 (24.33) 4.2 K, g_1 = 2.1029 (17.29), g_2 = 2.0712 (9.65), g_3 =1.9907 (21.30)
2,$\{Mn^{II}(CN)_2Pc\cdot(Mn^{II}(acac)_2)_2\}^{2-}$ S = 5/2, S = 1/2, S = 5/2 (S = 9/2 at 2K)	$\chi_M T$ = 8.74 emu·K/mol at 300 K, Θ = -12 K (50-300 K) $\chi_M T$= 11.60 emu·K/mol at 2 K	ZFS, D = 0.0647, E = 0.0192 cm^{-1}, E/D = 0.298 For S =5/2 case. Central signal splits into three lines: g_1 = 2.0705 (39.2), g_2 = 1.7892 (33.2), g_3 = 1.5410 (94.7) at 20 K
3, $\{Mn^{II}(CN)_2Pc\cdot(Cp_3Gd^{III})_2\}^{2-}$ S = 7/2, S = 1/2, S = 7/2	$\chi_M T$= 15.01 emu·K/mol at 300 K	293 K, g_1 = 1.8699 (107, 97.5%), g_2 = 1.7119 (29.4), g_3 = 1.8562 (11.02) 4.2 K, g_1 = 1.8342 (242, 97.5%), g_2 = 1.7994 (20.54), g_3 =1.8529 (8.90), g_4 = 1.9359 (2.79)
4, $\{Mn^{II}(CN)_2Pc\cdot(Cp_3Nd^{III})_2\}^{2-}$ S = 3/2, S = 1/2, S = 3/2	$\chi_M T$ = 2.30 emu·K/mol at 300 K	293 K, g_1 = 2.0275 (28.80), g_2 = 2.0836 (10.51), g_3 = 2.1167 (7.52), g_4 = 2.0039 (0.32), g_5 = 2.0022 (0.72), 4.2 K, g_1 = 1.9740 (24.60), g_2 = 2.0519 (11.63), g_3 = 2.0936 (8.97), g_4 = 2.0012 (0.49), g_5 = 1.9983 (0.84) Signals with g_1 and g_2 have only about 0.1% of total intensity.
5, $\{Fe^{II}(CN)_2Pc\}^{2-}$ (S = 0)	-	EPR silent
6,$\{Fe^{II}(CN)_2Pc\cdot(Cp_3Nd^{III})_2\}^{2-}$ S = 3/2, S = 0, S = 3/2	$\chi_M T$ = 1.92 emu·K/mol at 300 K	-
7, $\{Fe^{II}(CN)_2(PcCl_{16})\}^{2-}$ (S = 0)	Diamagnetic, χ_0 = -0.001376 emu/mol Curie impurities 1.2% Calc. χ_0 by using Pascal constants -0.001734 emu/mol	EPR silent

$$\hat{H}_1 = -2J_1\left(\hat{\vec{S}}_1\cdot\hat{\vec{S}}_2 + \hat{\vec{S}}_1\cdot\hat{\vec{S}}_3\right) - 2J_2\left(\hat{\vec{S}}_2\cdot\hat{\vec{S}}_3\right)$$

where $\hat{\vec{S}}_1$ is Mn^{II} (S = 1/2) spin, $\hat{\vec{S}}_2$ and $\hat{\vec{S}}_3$ are Mn^{II} (S = 5/2) spins, J_1 is Mn^{II}(S = 1/2) - Mn^{II}(S = 5/2) exchange interaction, J_2 is Mn^{II}(S = 5/2) - Mn^{II}(S = 5/2) exchange interaction inside a trinuclear Mn_3 assembly.

$$\hat{H}_2 = -2J_1\left(\hat{\vec{S}}_1\cdot\hat{\vec{S}}_2 + \hat{\vec{S}}_1\cdot\hat{\vec{S}}_3\right),$$

where $\hat{\vec{S}}_1$ is Mn^{II} (S = 1/2) spin, $\hat{\vec{S}}_2$ and $\hat{\vec{S}}_3$ are Gd^{III} (S = 7/2) spins, J_1 is Mn^{II}(S = 1/2) - Gd^{III}(S=7/2) exchange interaction

Magnetic data for compound 1.

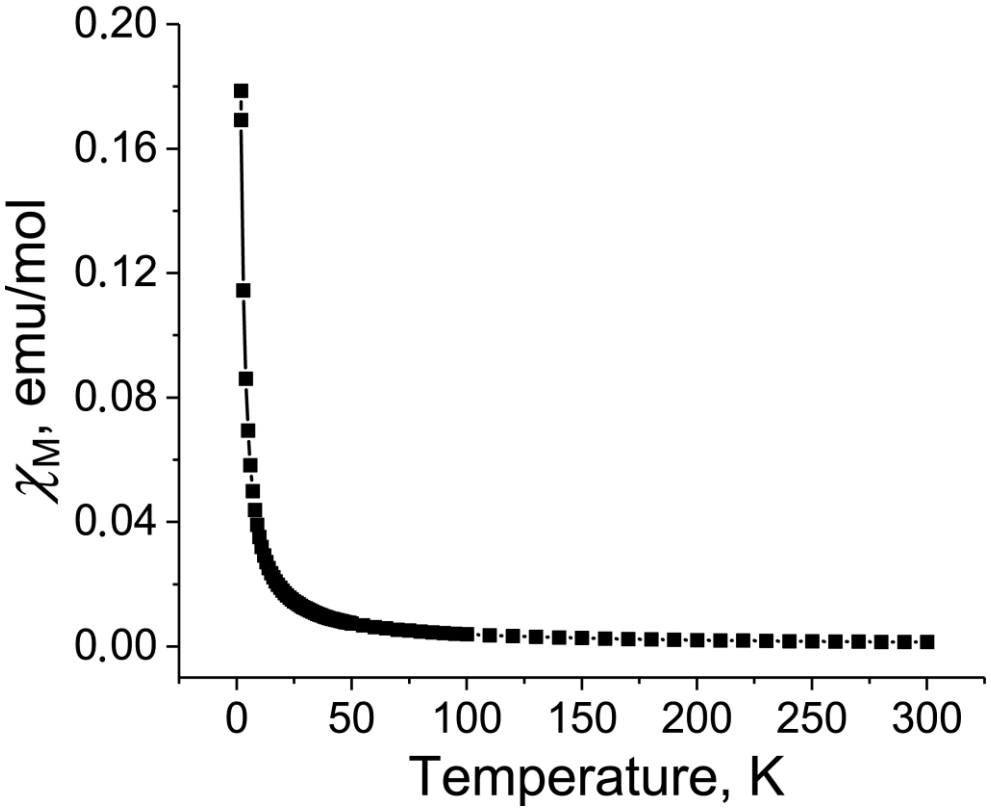

Figure S15. Temperature dependence of molar magnetic susceptibility of {Cryptand(K^+)}$_2${$Mn^{II}(CN)_2Pc$}$^{2-}$·$C_6H_4Cl_2$ (**1**).

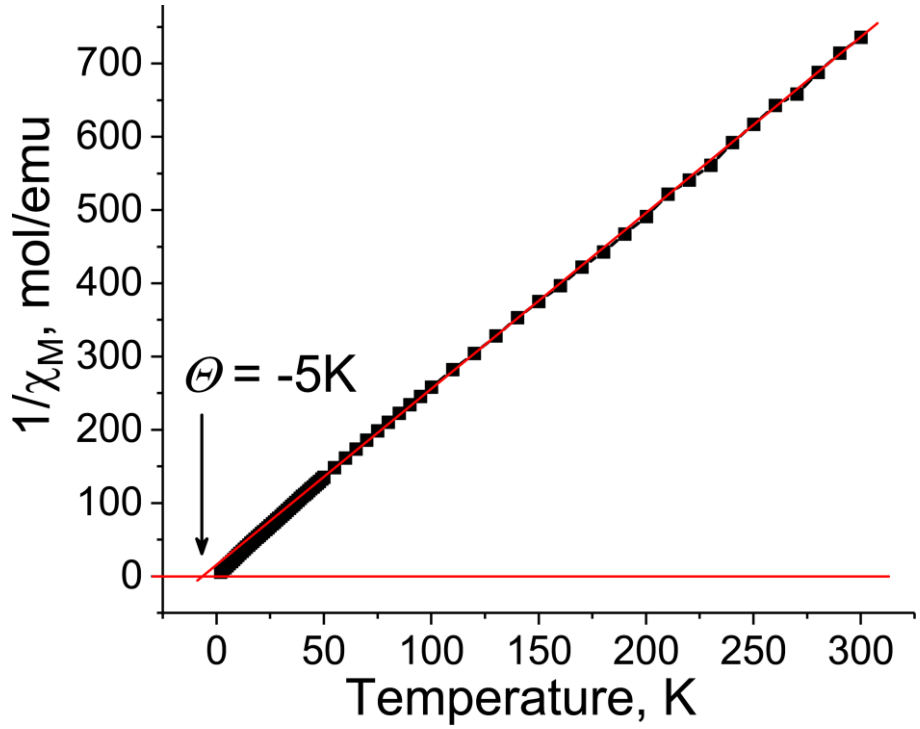

Figure S16. Temperature dependence of reciprocal molar magnetic susceptibility of {Cryptand(K^+)}$_2${$Mn^{II}(CN)_2Pc$}$^{2-}$·$C_6H_4Cl_2$ (**1**) which allows to determine Weiss temperature.

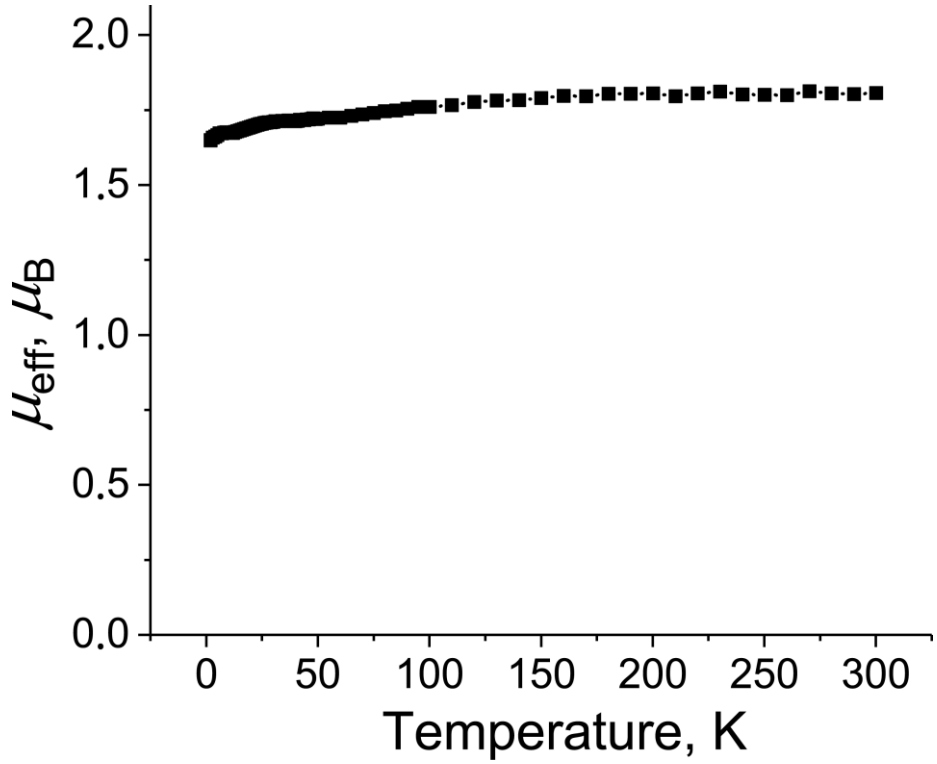

Figure S17. Temperature dependence for effective magnetic moment of $\{Cryptand(K^+)\}_2\{Mn^{II}(CN)_2Pc\}^{2-}\cdot C_6H_4Cl_2$ (**1**).

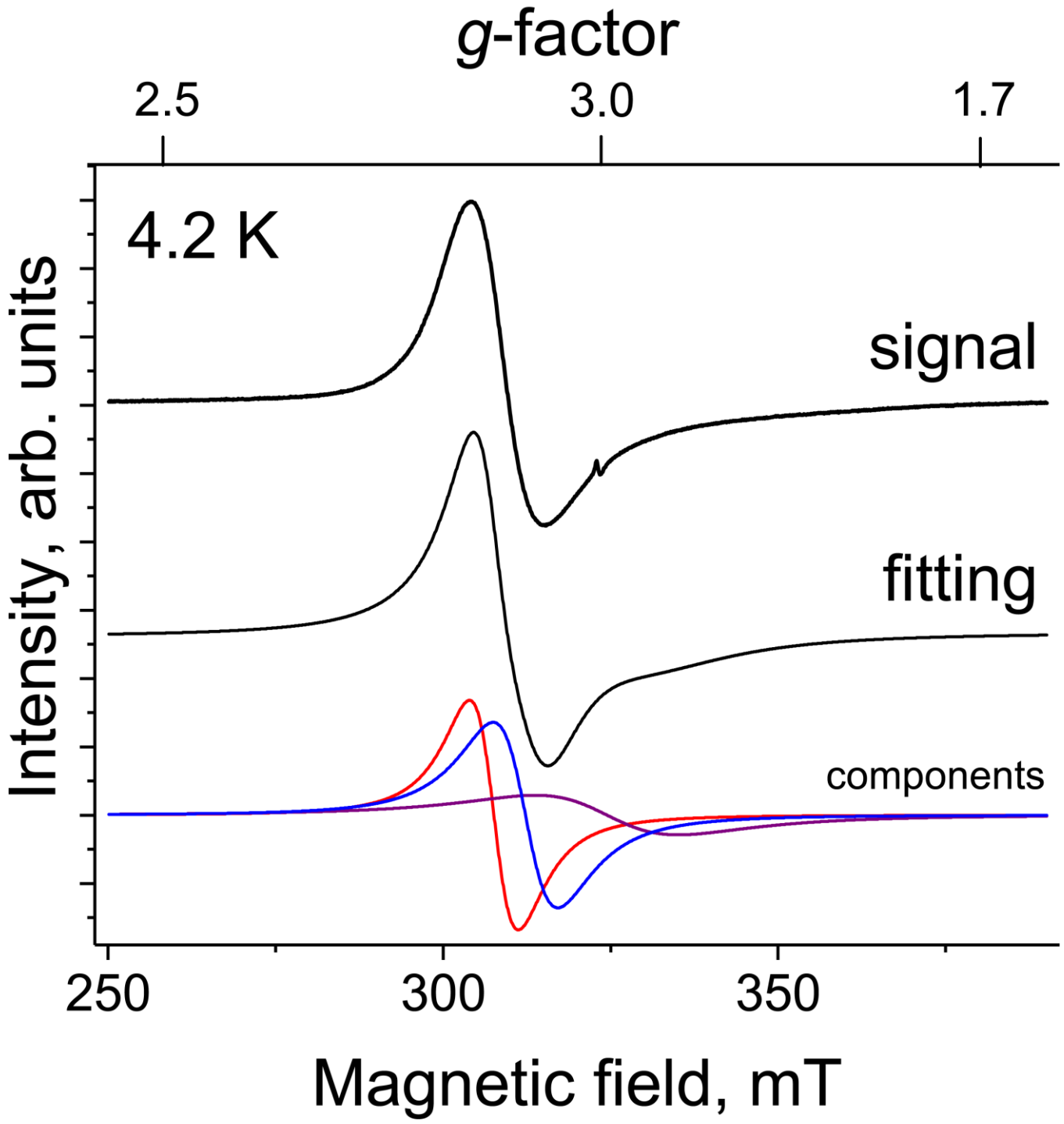

Figure S18. EPR spectrum of polycrystalline $\{Cryptand(K^+)\}_2\{Mn^{II}(CN)_2Pc\}^{2-}\cdot C_6H_4Cl_2$ (**1**) at 4.2 K. Fitting of the signal by three Lorentzian lines is shown below.

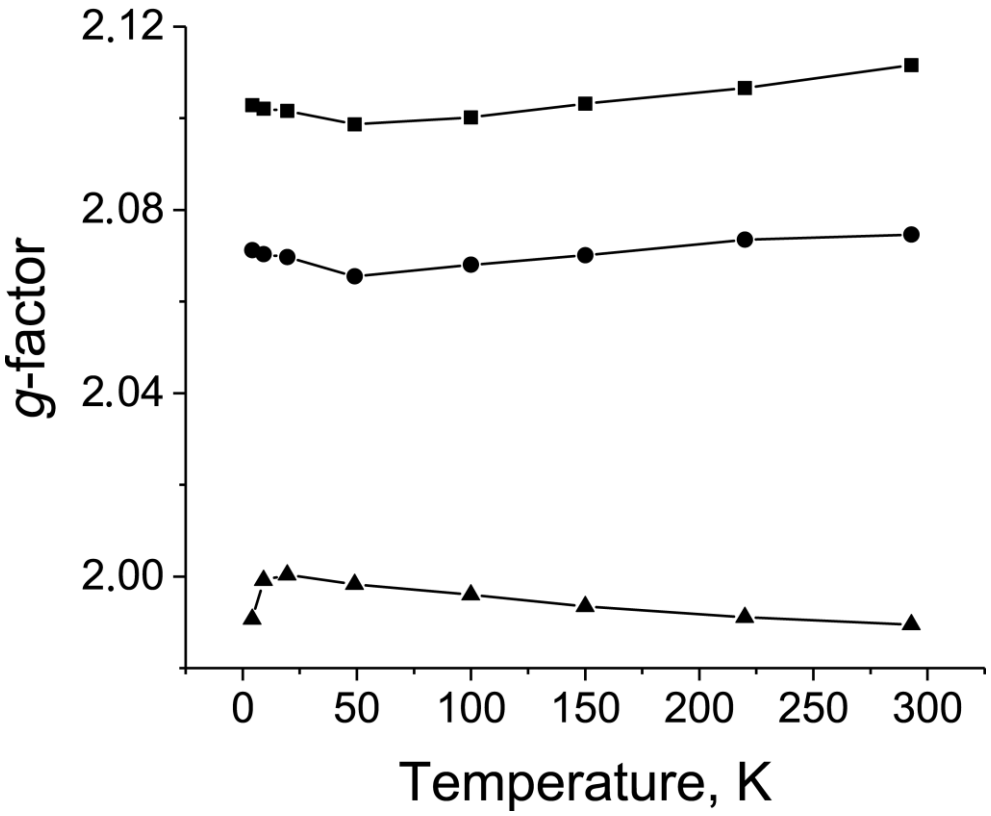

Figure S19. Temperature dependence of *g*-factors of three Lorentzian components of EPR signal from $\{Cryptand(K^+)\}_2\{Mn^{II}(CN)_2Pc\}^{2-}\cdot C_6H_4Cl_2$ (**1**).

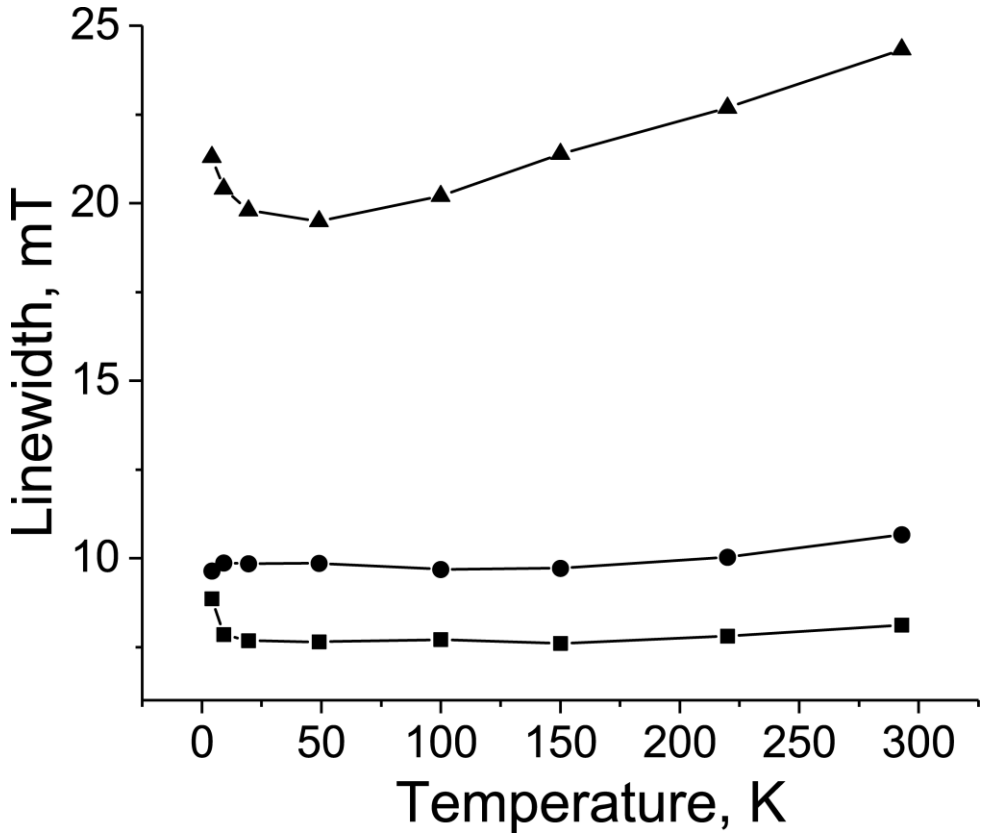

Figure S20. Temperature dependence of linewidth for three Lorentzian components of EPR signal from $\{Cryptand(K^+)\}_2\{Mn^{II}(CN)_2Pc\}^{2-}\cdot C_6H_4Cl_2$ (**1**).

Magnetic data for compound 2

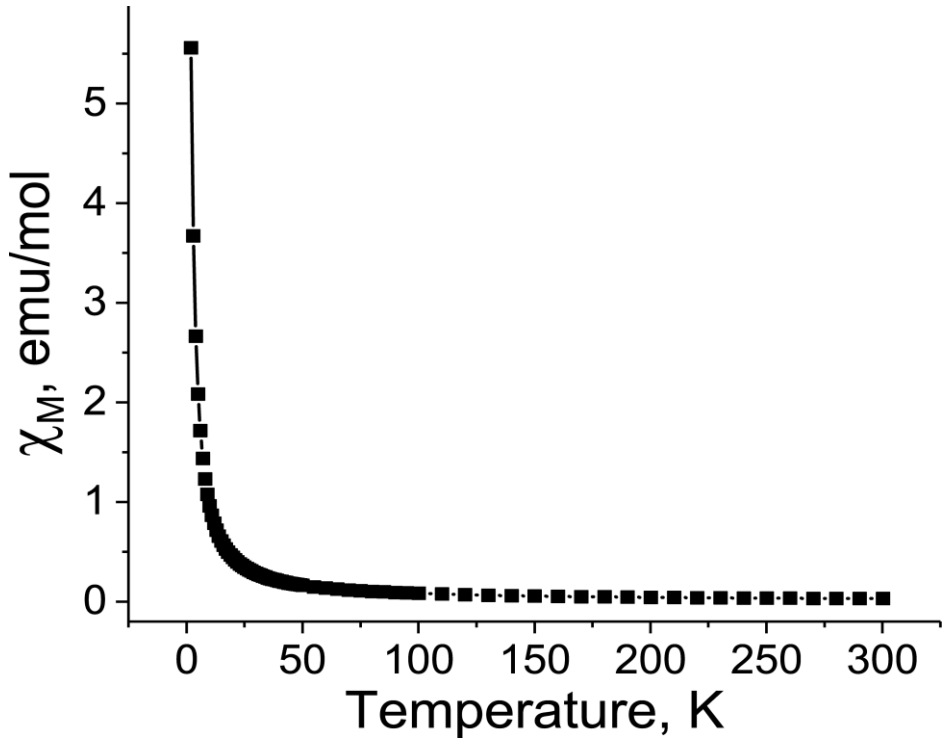

Figure S21. Temperature dependence of molar magnetic susceptibility of {Cryptand(K)}$_2$·{Mn^{II}(CN)$_2$Pc·[Mn^{II}(acac)$_2$]$_2$}·5C$_6$H$_4$Cl$_2$ (**2**).

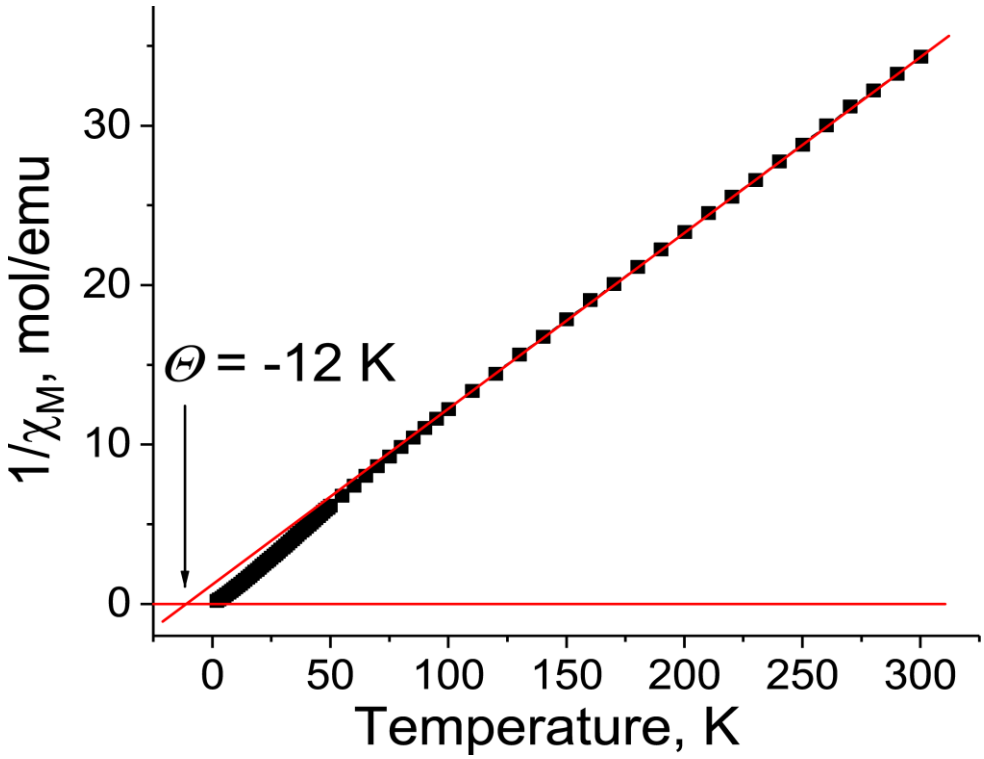

Figure S22. Temperature dependence of reciprocal molar magnetic susceptibility of {Cryptand(K)}$_2$·{Mn^{II}(CN)$_2$Pc·[Mn^{II}(acac)$_2$]$_2$}·5C$_6$H$_4$Cl$_2$ (**2**).

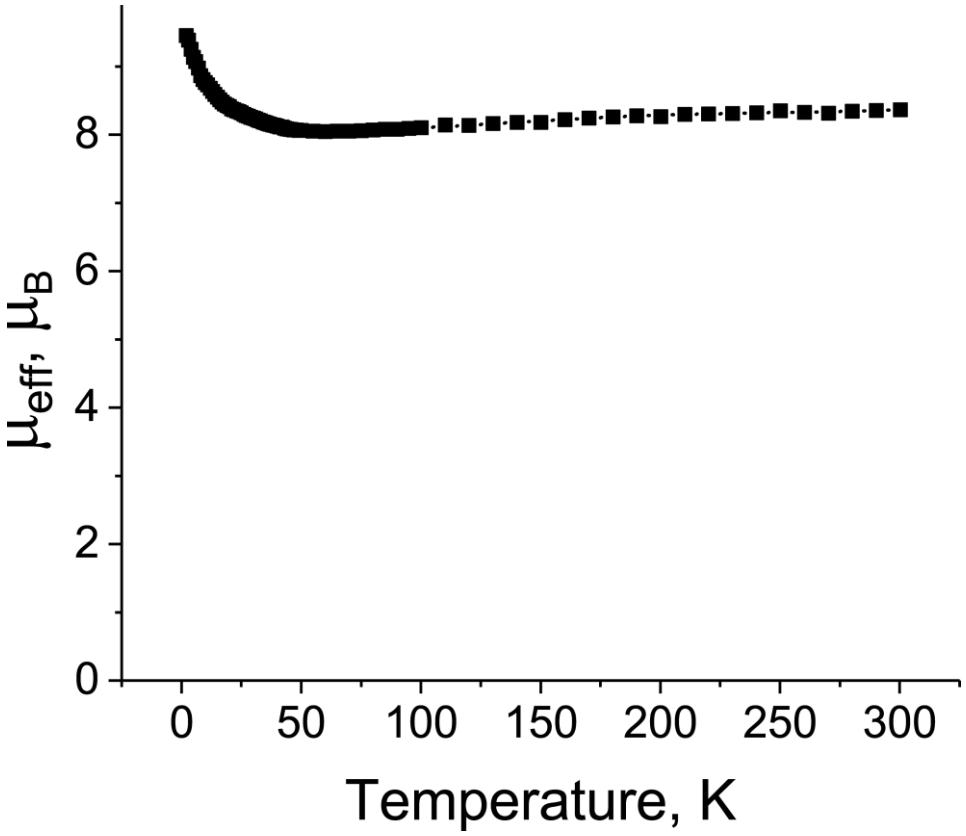

Figure S23. Temperature dependence of effective magnetic moment of $\{Cryptand(K)\}_2 \cdot \{Mn^{II}(CN)_2Pc \cdot [Mn^{II}(acac)_2]_2\} \cdot 5C_6H_4Cl_2$ (**2**) in the FC conditions.

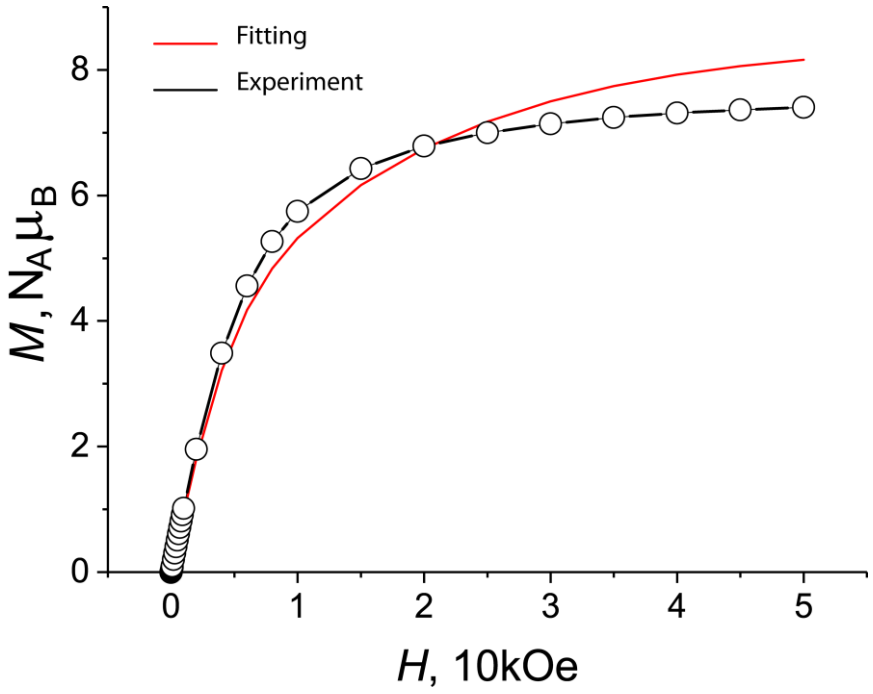

Figure S23a. Magnetization of **2** in $N_A\mu_B$ *vs* magnetic field up to 5T (black line is a guide to the eye) and fitting of these data by using PHI program (red curve).

Magnetic data for 3

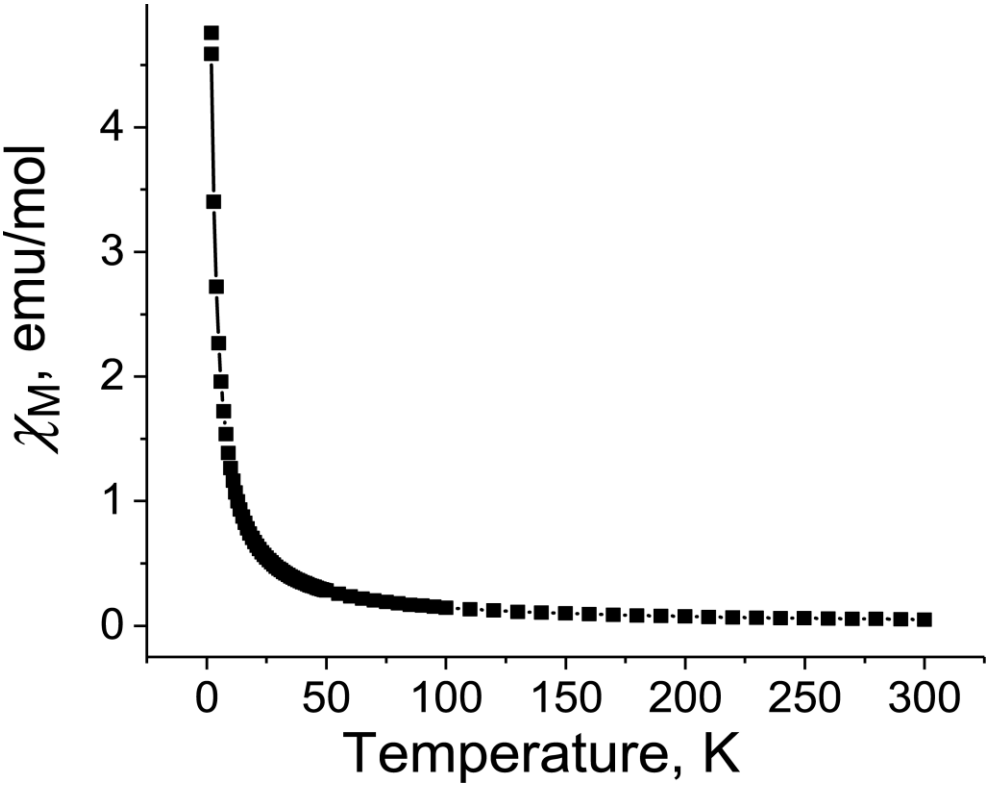

Figure S24. Temperature dependence of molar magnetic susceptibility of {Cryptand(K)}$_2${$Mn^{II}(CN)_2Pc\cdot(Cp_3Gd^{III})_2$}$\cdot 4C_6H_4Cl_2$ (**3**).

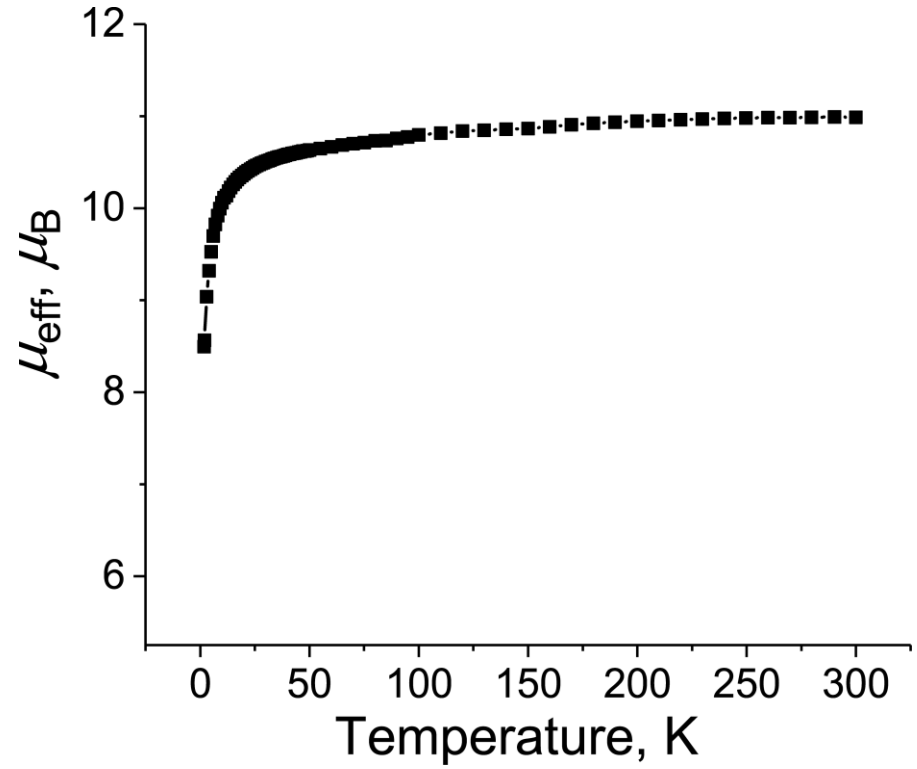

Figure S25. Temperature dependence of effective magnetic moment of $\{Cryptand(K)\}_2\{Mn^{II}(CN)_2Pc\cdot(Cp_3Gd^{III})_2\}\cdot 4C_6H_4Cl_2$ (**3**).

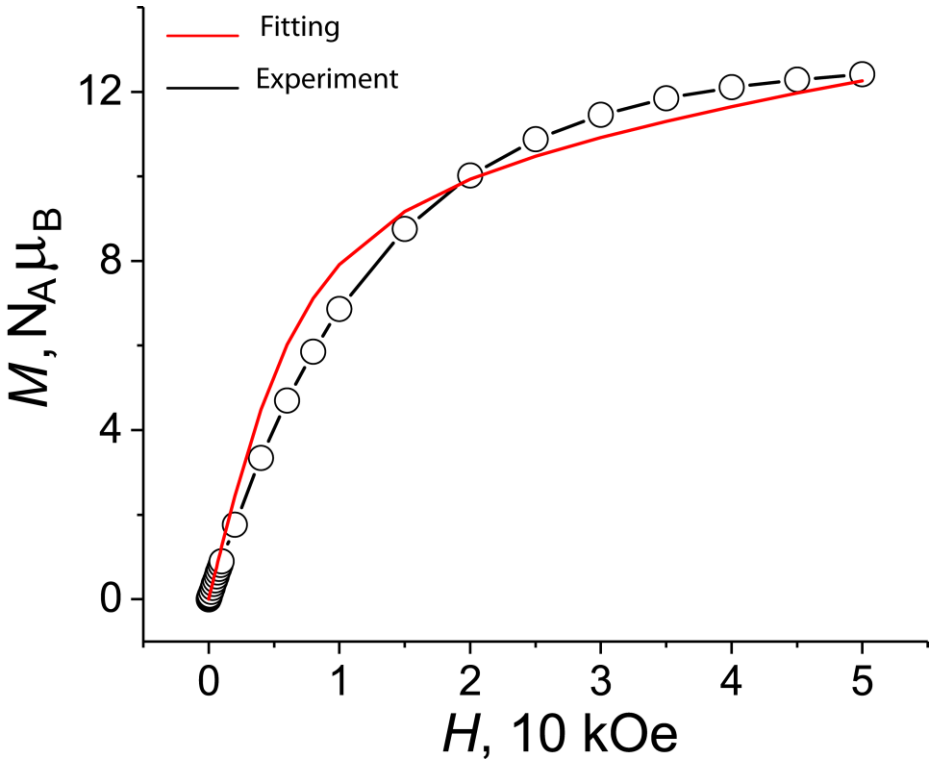

Figure S25a. Magnetization of **3** in $N_A\mu_B$ *vs* magnetic field up to 5T (black line is a guide to the eye) and fitting of these data by using PHI program (red curve).

EPR spectra of complex 3

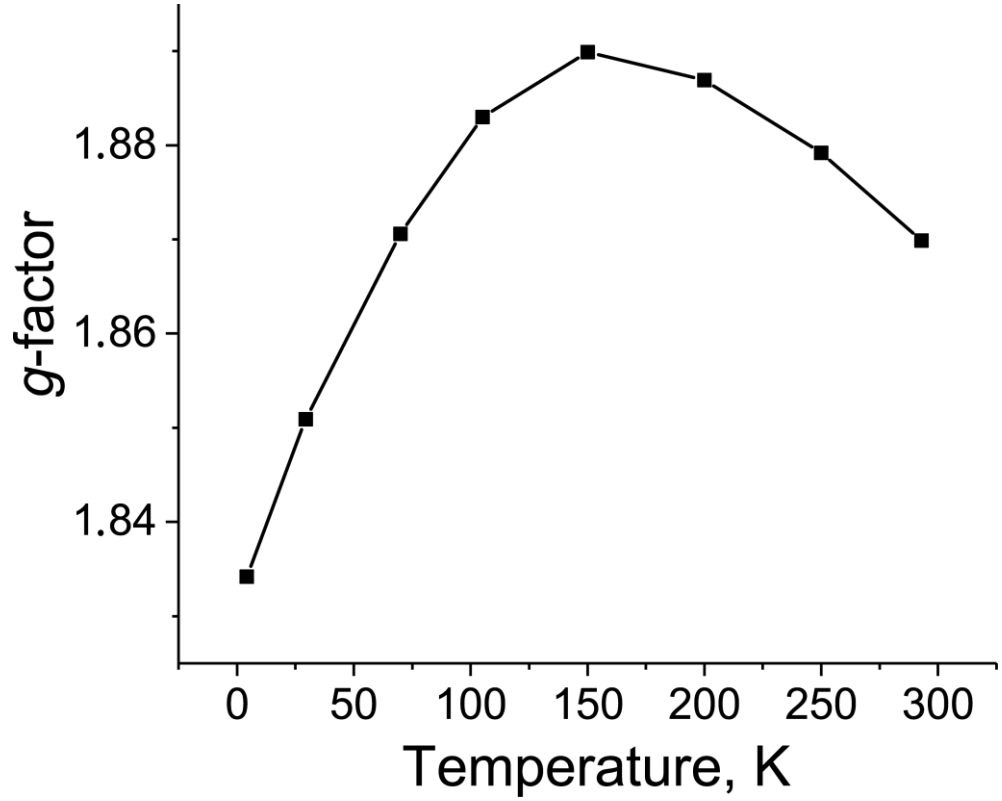

Figure S26. Temperature dependence of *g*-factor for broad EPR signal of **3.**

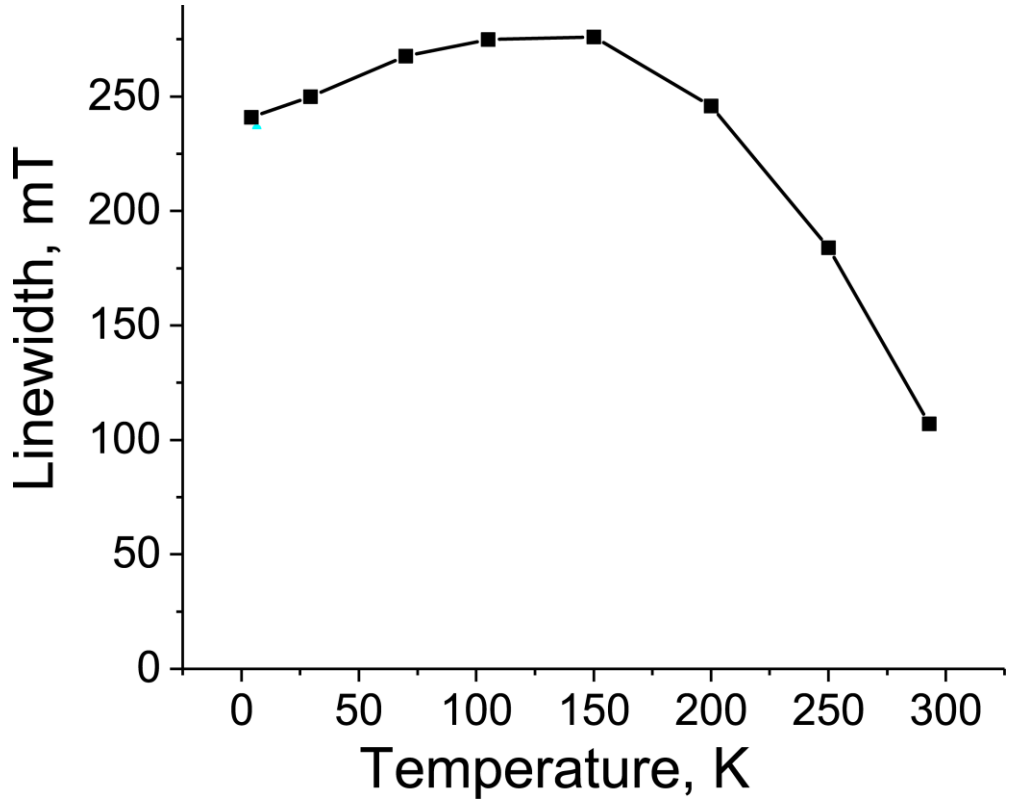

Figure S27. Temperature dependence of linewidth for broad EPR signal of **3.**

Magnetic data for complex 4.

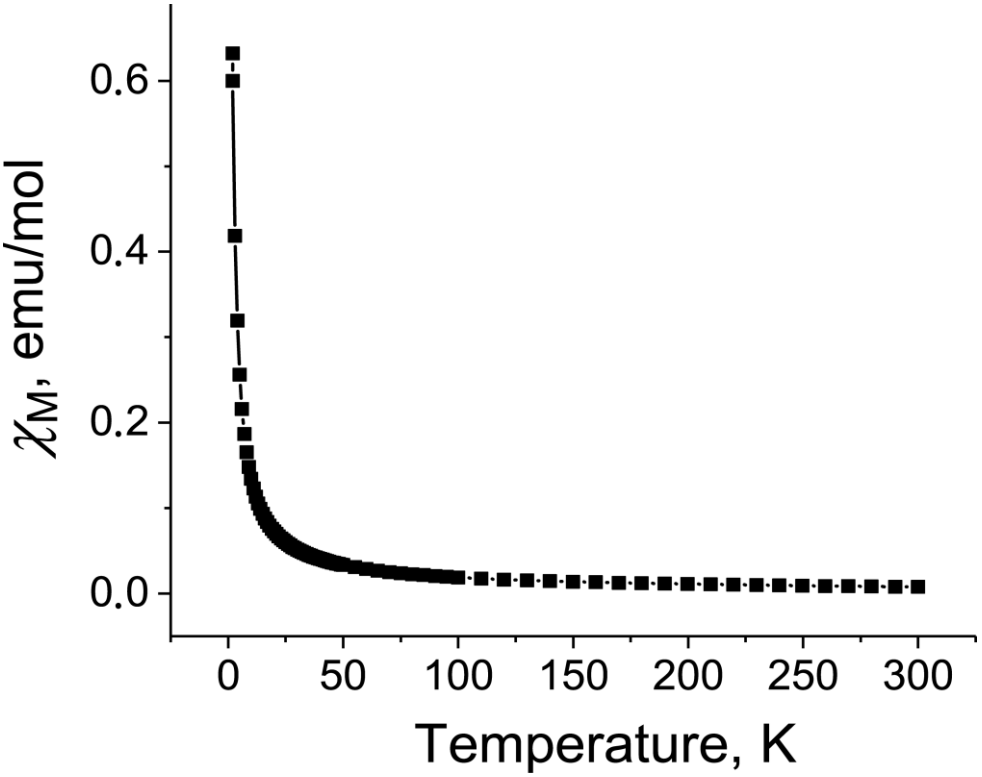

Figure S28. Temperature dependence of molar magnetic susceptibility of {Cryptand(K)}$_2${Mn^{II}(CN)$_2$Pc·(Cp$_3$Nd^{III})$_2$}·4C$_6$H$_4$Cl$_2$ (**4**).

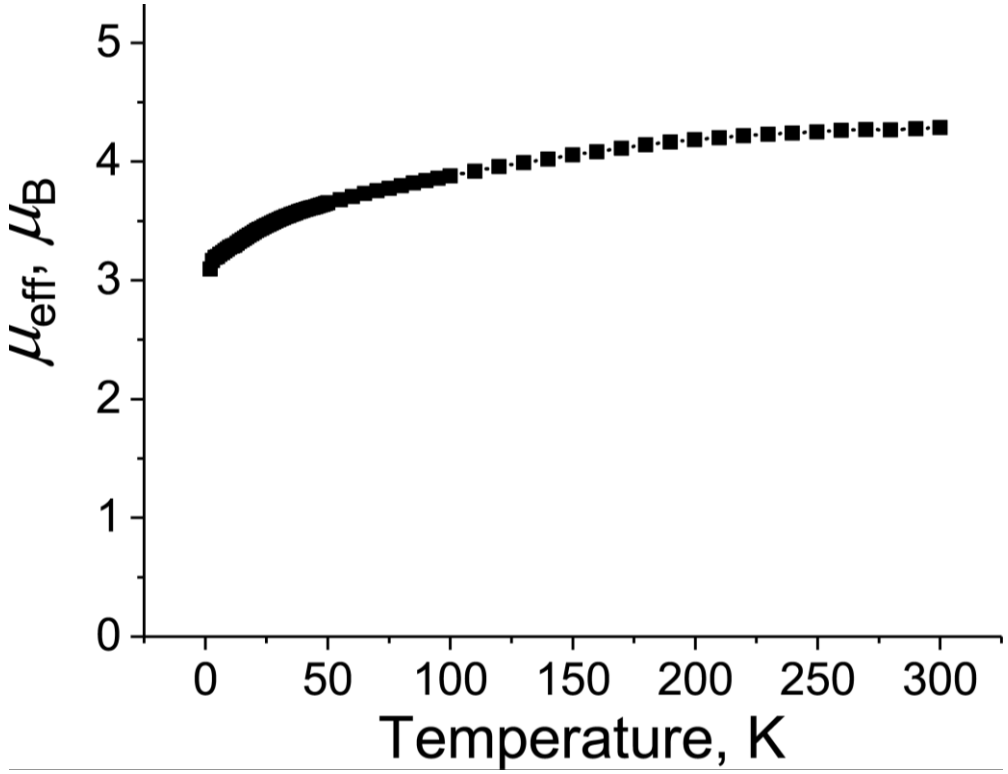

Figure S29. Temperature dependence of effective magnetic moment of {Cryptand(K)}$_2${Mn^{II}(CN)$_2$Pc·(Cp$_3$Nd^{III})$_2$}·4C$_6$H$_4$Cl$_2$ (**4**).

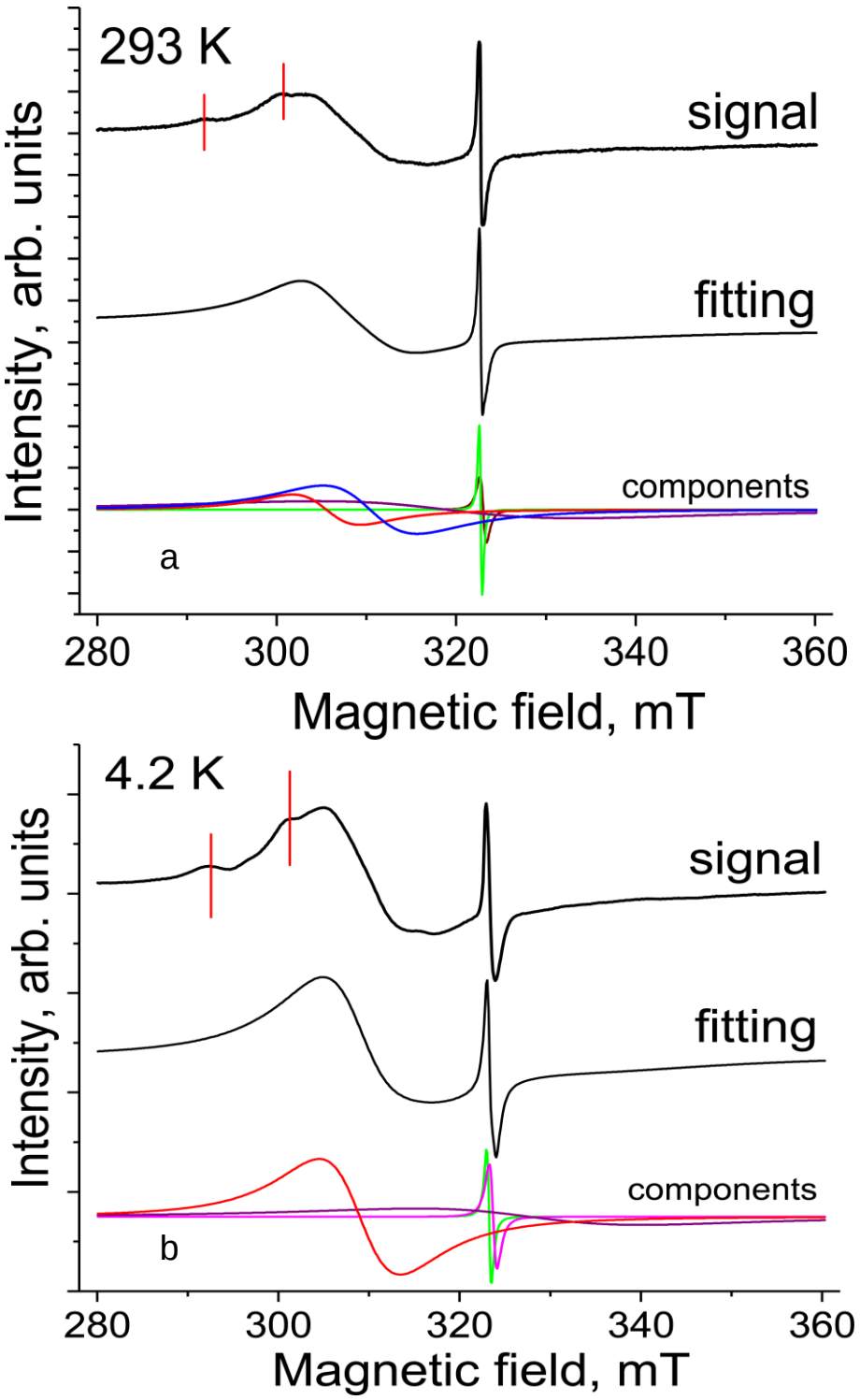

Figure S30. EPR spectra of polycrystalline **4** at 293 and 4.2 K. Fitting of the signal by five Lorentzian components is shown below. Red bars show additional features which can be attributed to non-resolved ZFS.

Magnetic data for 6

\

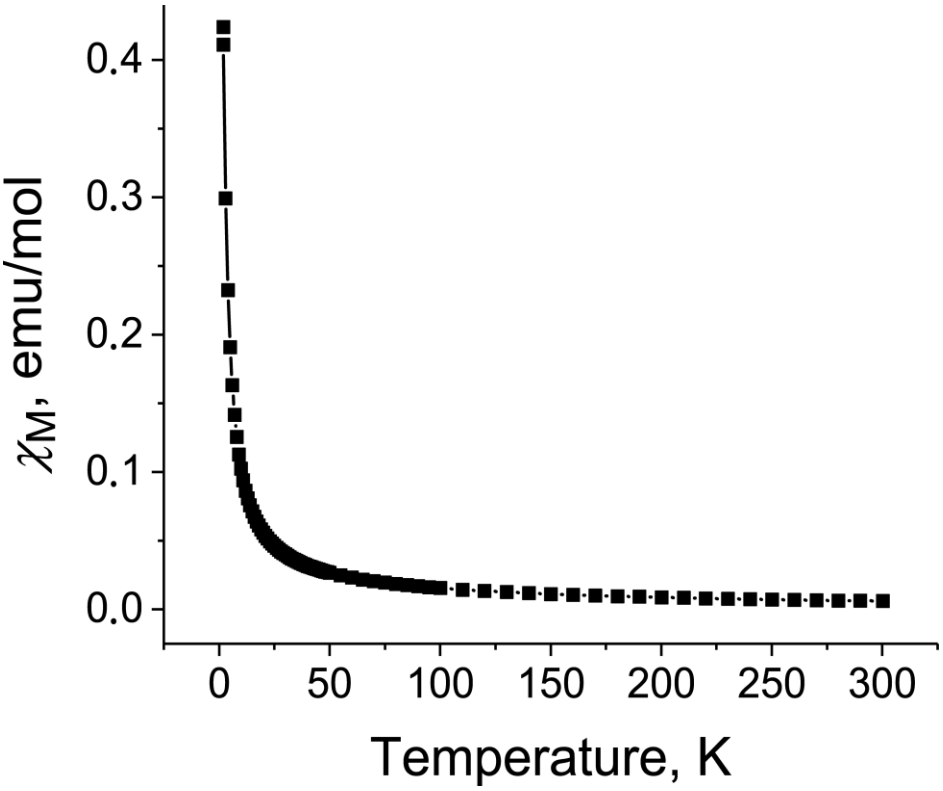

Figure S31. Temperature dependence of molar magnetic susceptibility of {Cryptand(K)}$_2${Fe^{II}(CN)$_2$Pc·(Cp$_3$Nd^{III})$_2$}·4C$_6$H$_4$Cl$_2$ (**6**).

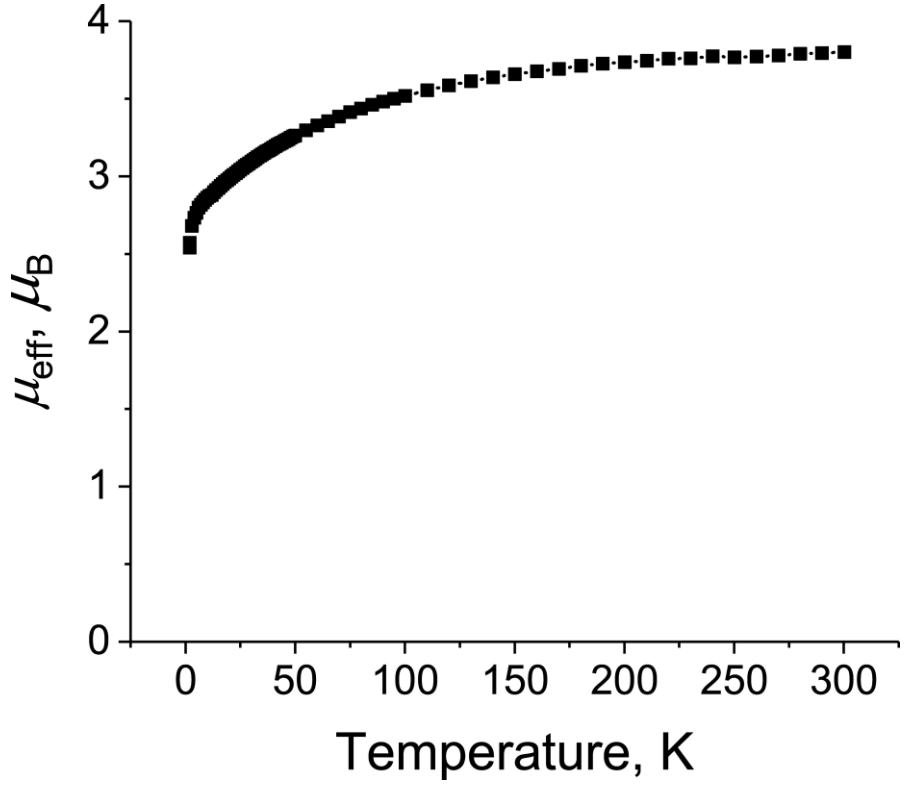

Figure S32. Temperature dependence of effective magnetic moment of {Cryptand(K)}$_2${Fe^{II}(CN)$_2$Pc·(Cp$_3$Nd^{III})$_2$}·4C$_6$H$_4$Cl$_2$ (**6**).

Magnetic data for 7

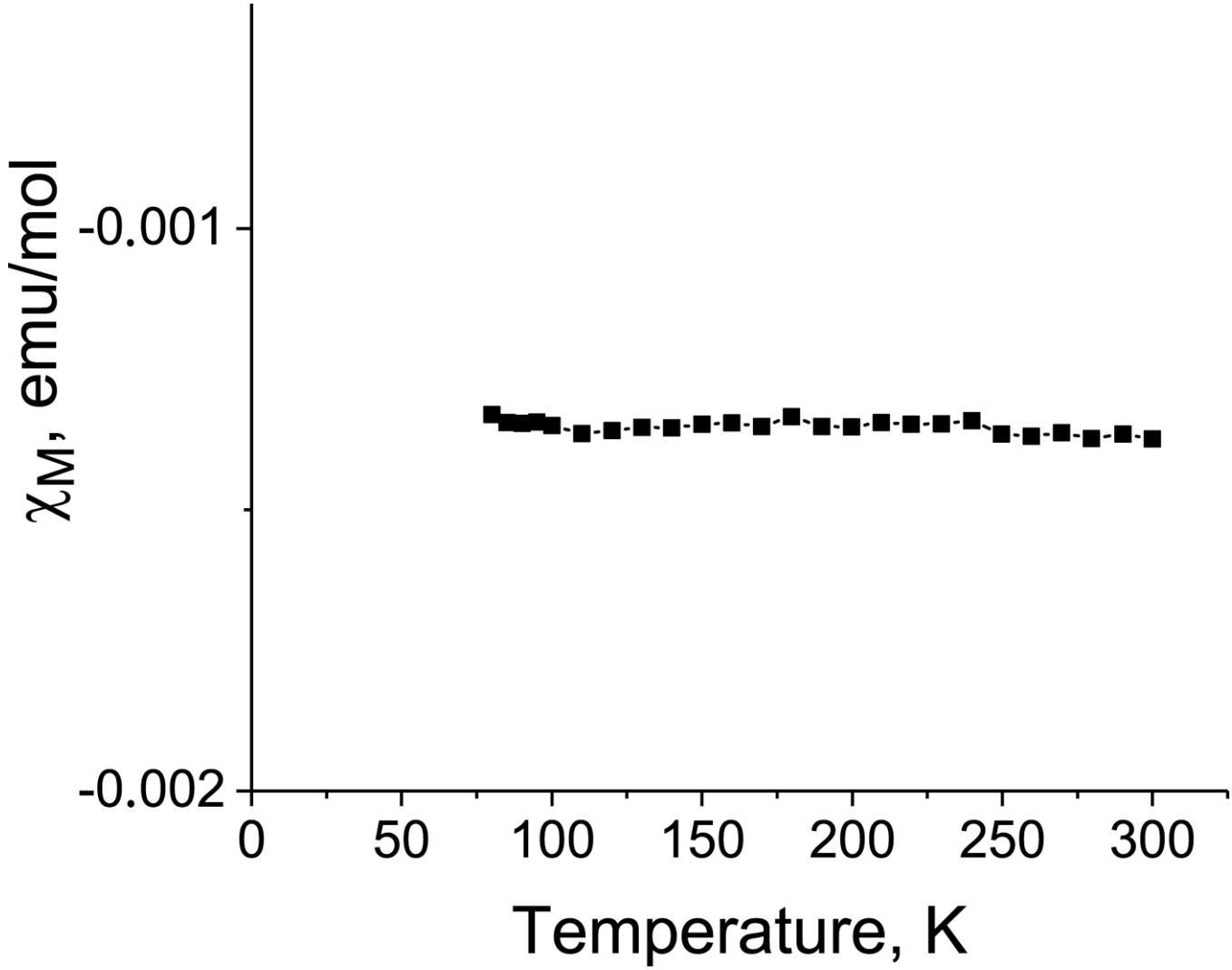

Figure S33. Temperature dependence of molar magnetic susceptibility of polycrystalline Cryptand(K)}$_2${$Fe^{II}(CN)_2(PcCl_{16})$}·$2C_6H_4Cl_2$ (**7**) in 70-300 K range.

Theoretical calculations

Optimization of the molecular structures was performed using the PBE exchange-correlation functional[4] and with the extended basis set Fe, Mn: [9s9p8d/5s5p4d], N,C: [5s5p2d/3s3p2d], H :[5s1p/3s1p] for the valence electrons and the SBK pseudopotential[5] implemented in the PRIRODA packag[6]. The Hirschfeld method[7] was used to calculate atomic charges. Electronic spectra are estimated using results of TDDFT calculations for energies and oscillator strengths of electronic transitions at fixed linewidth of 25 nm of Lorents peaks. All calculations were performed at Joint Supercomputer Center of the Russian Academy of Sciences.

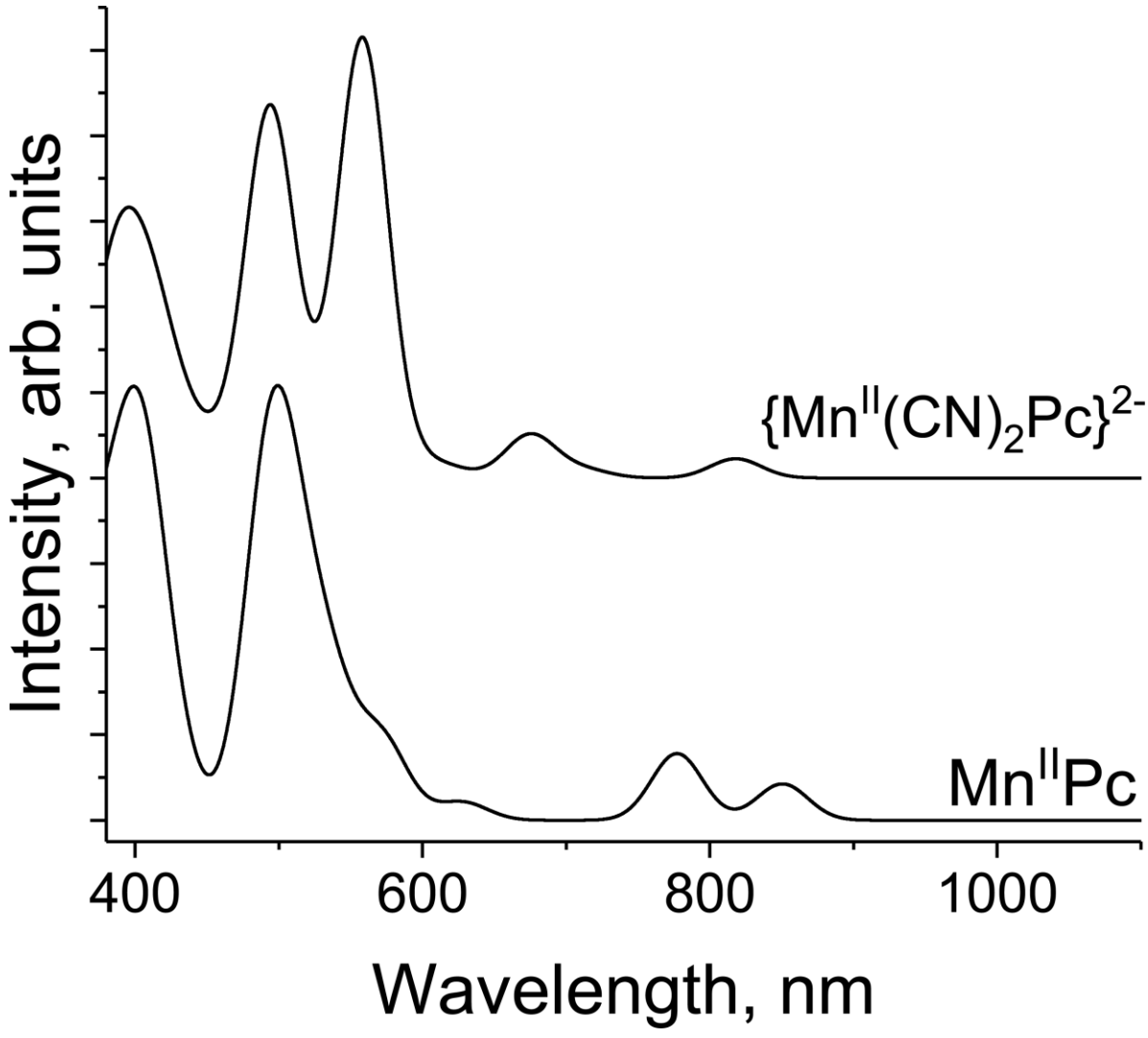

Fig. S34. Calculated spectra of pristine $Mn^{II}Pc$, its dicyano-complex $\{Mn^{II}(CN)_2Pc\}^{2-}$.

Optical spectra.

Calculated optical spectra of pristine $Mn^{II}Pc$ and its dicyano complex $\{Mn^{II}(CN)_2Pc\}^{2-}$ are shown in Fig. S37. The Soret and the Q-bands are manifested at 400 and 500 nm (the Q-band is strongly blue shifted relative to the experimental spectrum by about 230 nm). Low-energy bands at 780 and 856 nm are not manifested in the spectrum most probably due to low intensity. Formation of dicyano complex $\{Mn^{II}(CN)_2Pc\}^{2-}$ splits the Q-band into two bands positioned at 490 and 554 nm and this splitting is similar to that in experimental spectrum of **1** when the Q-band at 736 nm is split into two bands at 684 and 805 nm. Low-energy bands at 675 and 818 nm decrease in intensity at cyanation and are not manifested in the experimental spectrum.

Calculated molecular structures.

States with a total spin of 11/2 and 9/2, which differ in the orientation of a spin of the central Mn(II) atom (S =1/2), are generated for the $\{Mn^{II}(CN)_2Pc\cdot(Mn^{II}(acac)_2)_2\}^{2-}$ dianions. According to the calculations high-spin state of the system is lower in energy by 16.2 meV in comparison with low-spin state. Optimization of a neutral adduct with two counter cations: $\{Cryptand(K^+)\}_2\{Mn^{II}(CN)_2Pc\cdot(Mn^{II}(acac)_2)_2\}^{2-}$ shows their small effect on the geometry of trinuclear Mn complex (see Fig. S42). But there is a pronounced effect on the energy gap: a system with spin 11/2 has an energy less by 7.7 meV than that with spin 9/2. Since the accuracy of calculated total energies is 0.0001 a.u., or 2.7 meV. The energy gap predicted, 7.7 ± 5.4 meV or 89 ± 63 K, has a large error. To diminish this error it is necessary to use direct methods of calculation of small constants of magnetic coupling.

The D_{4h} symmetry of $\{Mn^{II}(CN)_2Pc\}^{2-}$ (Fig. S39) without C_2 distortion, which is found for $Mn^{II}Pc$ in quartet state (Fig. S38), shows that unpaired d electron of $\{Mn^{II}(CN)_2Pc\}^{2-}$ occupies xy orbital. The overlapping of this orbital with π orbitals of axial CN ligands coordinated to magnetic centers is symmetry forbidden. In this case ferromagnetic coupling is expected for the $\{Mn^{II}(CN)_2Pc\cdot(Mn^{II}(acac)_2)_2\}^{2-}$ dianions[8]. However angular coordination of $Mn^{II}(acac)_2$ units to cyano groups disturbs pure π symmetry of its frontier orbitals and favors enhancement of antiferromagnetic contribution into the magnetic coupling constant. The increase of antiferromagnetic contribution in the

cationic surrounding probably is due to considerable electron density transfer of 0.25 to each {Cryptand(K^+)} unit. As a result, the charge of the CN ligands becomes -0.220 in netral structure (Fig. S42) instead of -0.234 in $\{Mn^{II}(CN)_2Pc\cdot(Mn^{II}(acac)_2)_2\}^{2-}$ and side-on dispositions of the cations lead to further perturbation of symmetry of π orbitals According to the experiment data low spin S = 9/2 state is formed in the trinuclear assemblies and interaction between Mn^{II} (S = 5/2) and Mn^{II} (S =1/2) centers is clearly antiferromagnetic and we can assign this effect to the Coulomb interactions in the crystal lattice. Indeed, gap decreases nearly two times in the structure with two counter cations but in real crystal structure each dianionic assembly is surrounded by six such cations. However, this structure is too huge for the calculations.

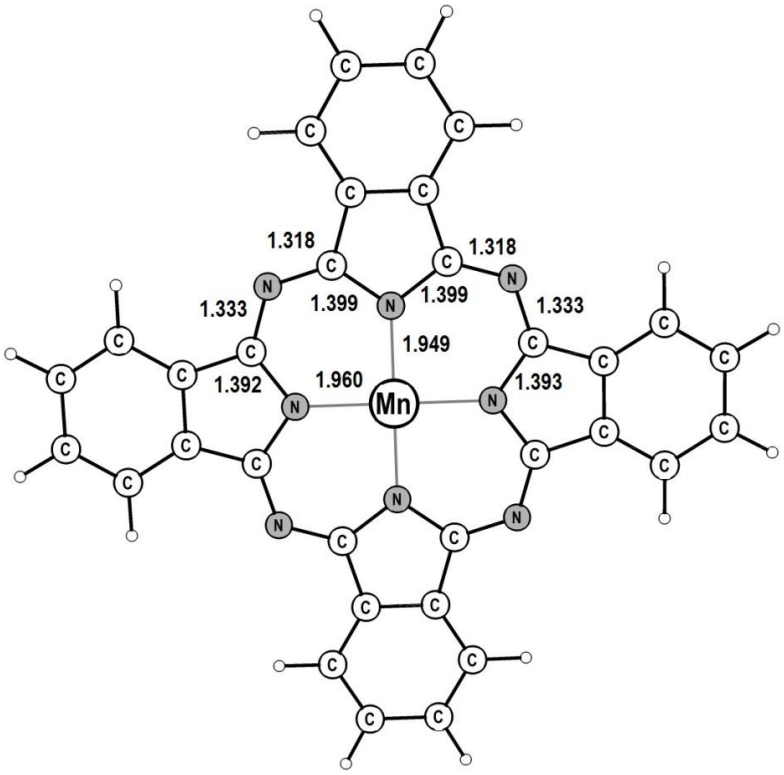

Fig. S35. Calculated structure of $Mn^{II}Pc$.

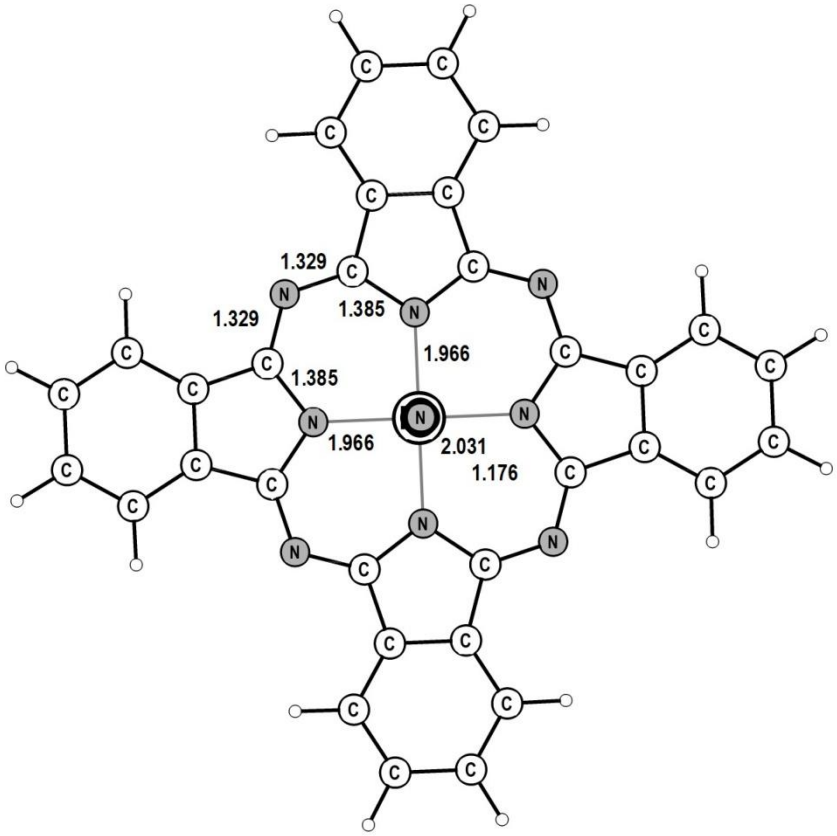

Fig. S36. Calculated structure of the $\{Mn^{II}(CN)_2Pc\}^{2-}$ dianion in doublet ground state.

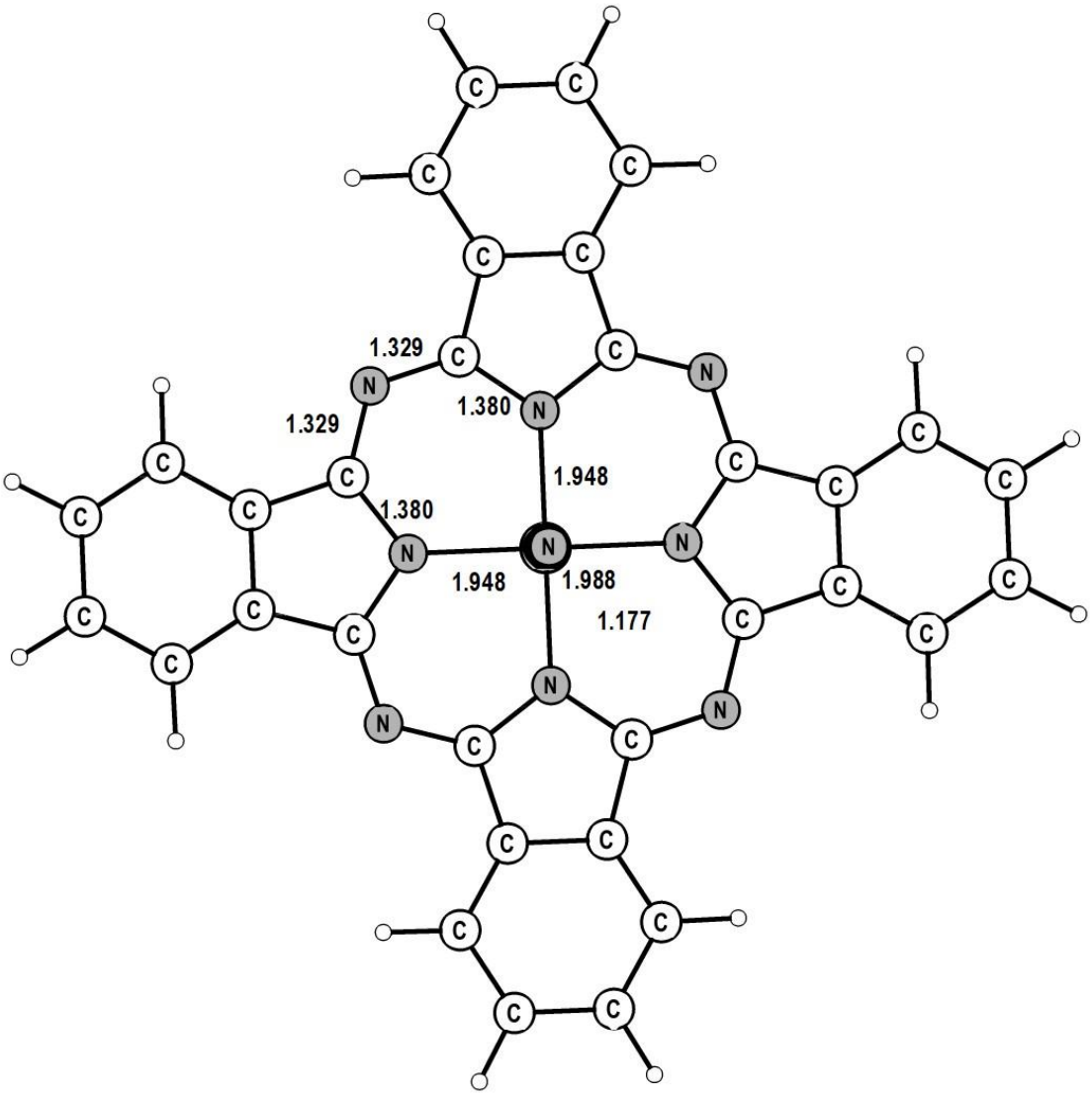

Fig. S37. Calculated structure of the $\{Fe^{II}(CN)_2Pc\}^{2-}$ dianion in singlet ground state.

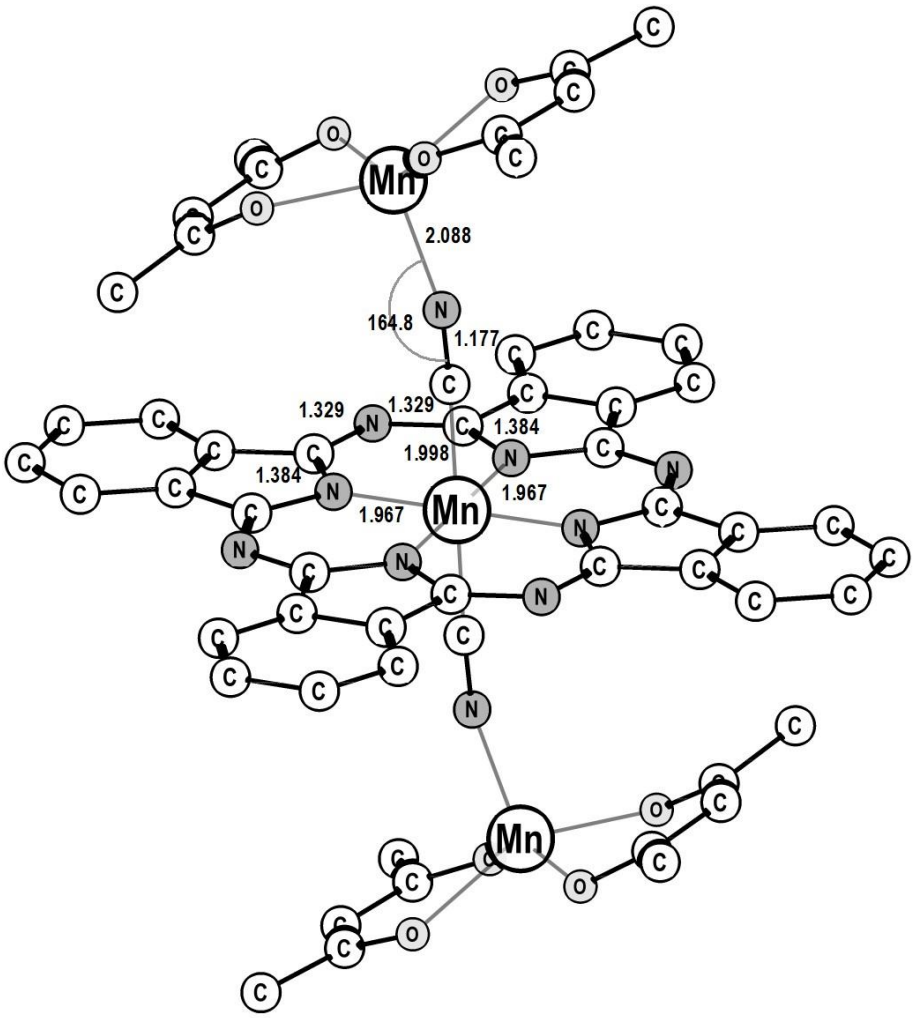

Fig. S38. Calculated structure of the $\{Mn^{II}(CN)_2Pc(Mn^{II}(acac)_2)_2\}^{2-}$ dianion in high-spin state (S =11/2). Hydrogen atoms are omitted for clarity.

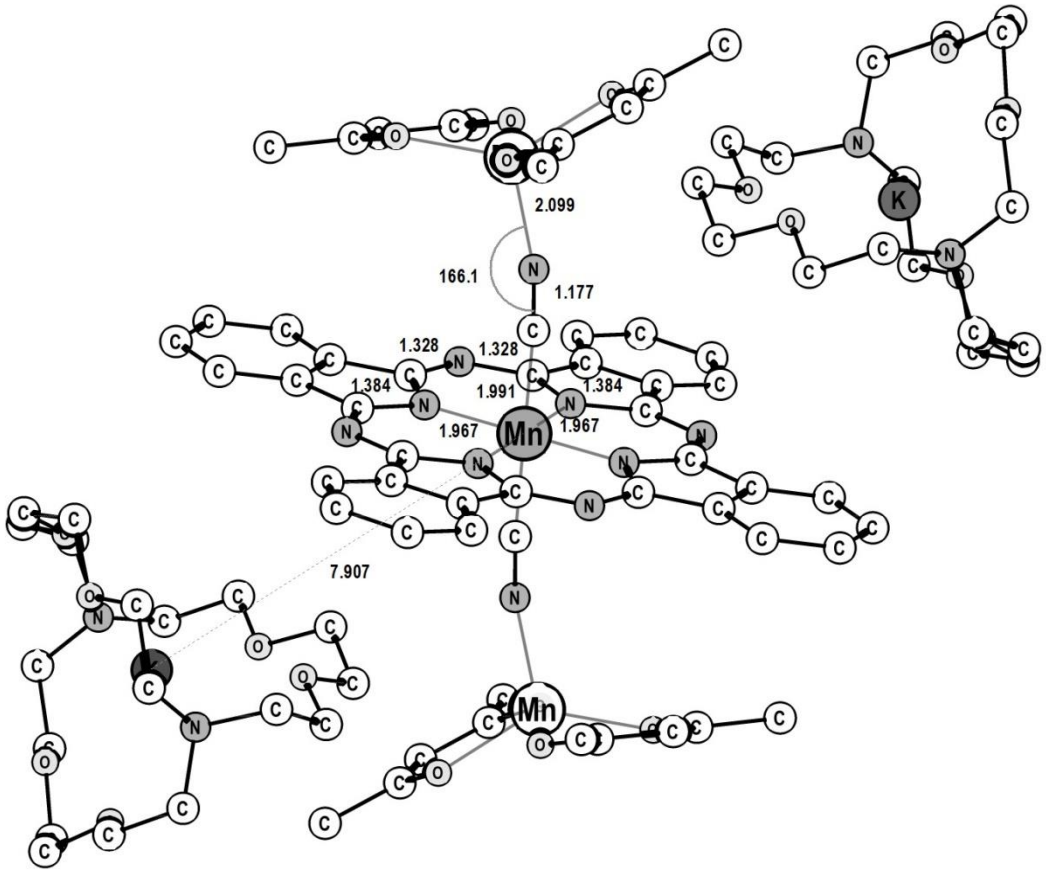

Fig. S39. Optimized structure of the $\{Mn^{II}(CN)_2Pc(Mn^{II}(acac)_2)_2\}^{2-}$ dianion in high-spin state (S =11/2) in cationic surrounding from two {Cryptand(K^+)} cations. The (K^+)-Mn^{II} distances found are close to that in the experimental crystal structure of **2**. Hydrogen atoms are omitted for clarity.

References.

1. D. V. Konarev, A. V. Kuzmin, A. F. Shestakov, I. A. Rompanen, R. N. Lyubovskaya, *Dalton Trans*, 2020, **49**, 16801.
2. G. M. Sheldrick, *Acta Crystallogr.,Sect. A: Fundam. Crystallogr*. 2008, **64**, 112.
3. D. V. Konarev, A. V. Kuzmin, S. V. Simonov, S. S. Khasanov, A. Otsuka, H. Yamochi, G. Saito, R. N. Lyubovskaya, *Dalton Trans*. 2012, **41**, 13841.
4. J. P. Perdew, K. Burke, M. Ernzerhof, *Phys. Rev. Lett*.1996, **77**, 3865.
5. W. J. Stevens, H. Basch, M. Krauss, *J. Chem. Phys*.,1984, **81**, 6026
6. D. N. Laikov, *Chem. Phys. Lett*.,1997, **281**, 151.
7. F. L. Hirshfeld, *Theor. Chim. Acta* 1977, **44**, 129.
8. Oliver Kahn: Molecular magnetism. VCH-Verlag, Weinheim, New York 1993. ISBN 3-527-89566-3, p. 380.

Cartesian coordinates of the optimized structures

$Mn^{II}Pc$, *S*=3/2

25	-0.00003941	-0.00013151	0.00000189
7	1.52552293	1.18791794	0.24090239
7	1.35044255	1.67687928	2.62074280
7	-0.43584757	0.17365205	1.90328795
7	-2.41446349	-1.25296173	2.02605869
6	3.42668957	2.47622304	-0.16640066
6	4.52590227	3.13841677	-0.72244129
6	5.30240355	3.93425035	0.12915312
6	4.98697158	4.06205848	1.49685567
6	3.88513331	3.39895760	2.05164088
6	3.11029832	2.60558747	1.19948188
6	1.92059362	1.79420159	1.43860270
6	0.26706766	0.93142977	2.83642343
6	-0.36678045	0.79544541	4.12867569
6	-0.06521641	1.34168524	5.38670111
6	-0.89602595	1.00358758	6.45428876
6	-2.00529348	0.14034400	6.27912573
6	-2.30955373	-0.40474842	5.03228464
6	-1.47630496	-0.06754731	3.95341878
6	-1.49943980	-0.44271659	2.55738371
6	-2.42642362	-1.58887981	0.75196276
7	-1.52524388	-1.18839977	-0.24076044
7	-1.35046788	-1.67678687	-2.62071367
7	0.43606623	-0.17379725	-1.90320323
7	2.41487195	1.25246518	-2.02589500
6	-3.42532315	-2.47810960	0.16689353
6	-4.52420000	-3.14079842	0.72301812
6	-5.30048328	-3.93690770	-0.12851846
6	-4.98508049	-4.06464869	-1.49623232
6	-3.88357262	-3.40107525	-2.05110929
6	-3.10910182	-2.60723297	-1.19905749
6	-1.92028042	-1.79462544	-1.43846398
6	-0.26746950	-0.93078092	-2.83655273
6	0.36581564	-0.79407041	-4.12900612
6	0.06333620	-1.33908670	-5.38734416
6	0.89364825	-1.00034672	-6.45511533
6	2.00316405	-0.13744590	-6.27987564
6	2.30823375	0.40656061	-5.03275466
6	1.47541368	0.06881733	-3.95373016
6	1.49936040	0.44293181	-2.55742325
6	2.42726521	1.58767171	-0.75162678
1	4.76325368	3.03415026	-1.78159494
1	6.16778793	4.46517496	-0.27095565
1	5.61342795	4.68981226	2.13273189
1	3.63416844	3.49296817	3.10861472
1	0.79040462	2.00533337	5.51462220
1	-0.69135420	1.40999689	7.44622826
1	-2.63166373	-0.10008953	7.13985255
1	-3.16187840	-1.06981245	4.89047380

1	-4.76161318	-3.03651911	1.78215815
1	-6.16560505	-4.46819769	0.27167481
1	-5.61129382	-4.69271706	-2.13204048
1	-3.63281943	-3.49478916	-3.10816003
1	-0.79242147	-2.00254949	-5.51530972
1	0.68825467	-1.40579975	-7.44729721
1	2.62914124	0.10351251	-7.14074202
1	3.16062193	1.07154061	-4.89093592

$\{Mn^{II}(CN)_2Pc\}^{2-}$, $S = 1/2$

25	-0.00036251	0.00030485	0.00000501
7	1.54007325	1.19725604	0.24341019
7	1.34301127	1.67956141	2.62642632
7	-0.44026641	0.17844809	1.90824443
7	-2.41763507	-1.24334926	2.03104347
6	3.42668466	2.47253842	-0.16993082
6	4.53020802	3.13839486	-0.71857535
6	5.30980585	3.93606578	0.12897858
6	4.99284555	4.06534680	1.49948553
6	3.88933773	3.40038850	2.04951941
6	3.10866407	2.60262575	1.20318568
6	1.92044963	1.79238134	1.43447743
6	0.26041929	0.93581381	2.83147143
6	-0.37697391	0.80632238	4.13480885
6	-0.08199578	1.35215810	5.39066309
6	-0.91401891	1.02090147	6.46788531
6	-2.02058271	0.16039096	6.29320935
6	-2.31709088	-0.38606046	5.03786658
6	-1.48608265	-0.05570759	3.95968310
6	-1.50184437	-0.43394465	2.55328266
6	-2.42575270	-1.58558196	0.74683571
7	-1.85889044	2.52800621	-0.66756064
6	-1.17772713	1.60108367	-0.42144810
7	-1.54042013	-1.19682714	-0.24411844
7	-1.34412069	-1.67833538	-2.62716390
7	0.43947035	-0.17778084	-1.90824887
7	2.41884811	1.24232285	-2.03159323
6	-3.42561738	-2.47397801	0.16998653
6	-4.52873525	-3.14023463	0.71893112
6	-5.30891185	-3.93729400	-0.12866873
6	-4.99284880	-4.06563484	-1.49947715
6	-3.88975577	-3.40023869	-2.04981130
6	-3.10850854	-2.60308362	-1.20342067
6	-1.92114505	-1.79176074	-1.43510452
6	-0.26149733	-0.93467901	-2.83190120
6	0.37644054	-0.80581826	-4.13491793
6	0.08078710	-1.35047426	-5.39115437
6	0.91346513	-1.01973994	-6.46800284
6	2.02094837	-0.16050944	-6.29271218
6	2.31798302	0.38481140	-5.03700829
6	1.48612407	0.05519310	-3.95926653

6	1.50194059	0.43298597	-2.55257158
6	2.42685804	1.58430345	-0.74704179
1	4.76488984	3.03146571	-1.77922300
1	6.17652020	4.46706913	-0.27368644
1	5.61891836	4.69441310	2.13792412
1	3.63466499	3.49257427	3.10693226
1	0.77635136	2.01516030	5.51379514
1	-0.70579885	1.43280337	7.45898268
1	-2.65273938	-0.08173398	7.15172195
1	-3.16886779	-1.05267903	4.89096767
1	-4.76299319	-3.03360977	1.77970422
1	-6.17548562	-4.46841266	0.27415017
1	-5.61944178	-4.69413364	-2.13796407
1	-3.63599360	-3.49144937	-3.10752694
1	-0.77826390	-2.01248114	-5.51471773
1	0.70470802	-1.43054000	-7.45944739
1	2.65365609	0.08112659	-7.15095787
1	3.17017787	1.05079978	-4.88968894
6	1.17717318	-1.60022256	0.42165508
7	1.85894379	-2.52672262	0.66767778

$\{Fe^{II}(CN)_2Pc\}^{2-}$, $S = 0$

26	-0.00047307	0.00040251	-0.00013136
7	1.52629626	1.18551234	0.24127341
7	1.34091546	1.67327795	2.61984225
7	-0.43466786	0.17492042	1.89073276
7	-2.40950651	-1.24339680	2.02755837
6	3.41837246	2.46775529	-0.17002215
6	4.52071446	3.13193095	-0.72023904
6	5.30045256	3.93054495	0.12788107
6	4.98324274	4.06031920	1.49713769
6	3.87953622	3.39421748	2.04780838
6	3.10196862	2.59615381	1.20072757
6	1.91179027	1.78127094	1.42439915
6	0.25828632	0.92767919	2.81626640
6	-0.37493690	0.80364919	4.12556916
6	-0.07928895	1.35093144	5.37942730
6	-0.91228868	1.01928623	6.45702498
6	-2.01760628	0.15901620	6.28228985
6	-2.31350123	-0.38848995	5.02620812
6	-1.48117555	-0.05738287	3.95074928
6	-1.48923165	-0.43279096	2.54022343
6	-2.41123419	-1.57927379	0.74150290
7	-1.83323603	2.49614647	-0.65589022
6	-1.15211756	1.56809953	-0.41108204
7	-1.52607094	-1.18615547	-0.24100211
7	-1.34177513	-1.67228469	-2.62004229
7	0.43517276	-0.17576882	-1.89044493
7	2.41119933	1.24057353	-2.02657641
6	-3.41757719	-2.46909712	0.17044791
6	-4.52007081	-3.13315880	0.72050743

6	-5.30121401	-3.92971949	-0.12825353
6	-4.98523492	-4.05768506	-1.49797500
6	-3.88139358	-3.39170620	-2.04849689
6	-3.10240248	-2.59575833	-1.20076225
6	-1.91239383	-1.78066056	-1.42449508
6	-0.25852036	-0.92750705	-2.81624178
6	0.37533286	-0.80422271	-4.12529186
6	0.07819369	-1.34977481	-5.37952879
6	0.91163143	-1.01895876	-6.45704301
6	2.01840214	-0.16062511	-6.28190926
6	2.31564683	0.38530138	-5.02545569
6	1.48273220	0.05519954	-3.95013874
6	1.49136814	0.42975713	-2.53941508
6	2.41278861	1.57691166	-0.74074691
1	4.75491083	3.02501110	-1.78098930
1	6.16698124	4.46195535	-0.27472960
1	5.60880126	4.69017710	2.13535652
1	3.62473026	3.48610571	3.10521130
1	0.77862778	2.01453271	5.50240523
1	-0.70482238	1.43154802	7.44816801
1	-2.64995469	-0.08307235	7.14071432
1	-3.16487328	-1.05547445	4.87863907
1	-4.75364188	-3.02728442	1.78150128
1	-6.16801419	-4.46080374	0.27419621
1	-5.61198675	-4.68584803	-2.13668785
1	-3.62759211	-3.48185778	-3.10629270
1	-0.78089092	-2.01181692	-5.50259364
1	0.70296685	-1.42973394	-7.44854951
1	2.65113594	0.08081153	-7.14023350
1	3.16791639	1.05109641	-4.87771563
6	1.15275955	-1.56616140	0.41038527
7	1.83482042	-2.49362488	0.65482150

$\{Mn^{II}(CN)_2Pc(Mn^{II}(acac)_2)_2\}^{2-}$, $S = 11/2$

25	-0.00159860	0.00108751	-0.00214999
25	-0.84048387	-4.79876864	-1.83428504
8	1.19853494	-5.32468362	-1.87824331
8	-0.53645526	-4.26148655	-3.84860933
8	-2.85760800	-5.24246287	-2.32573302
8	-1.12429203	-6.28559469	-0.34502293
7	-0.32554408	-0.76805015	3.28487902
7	1.19110912	-0.73369173	1.37842811
7	3.23082556	-1.02088652	0.07733185
7	1.46155875	-0.08809563	-1.31399574
7	-0.80185166	-2.94262089	-0.87811501
6	-1.37992604	-0.27906191	2.64053092
6	0.84734670	-0.97713396	2.69659156
6	2.00505340	-1.51932218	3.39914442
6	2.19861738	-1.92821419	4.72374633
1	1.38338132	-1.86376787	5.44617571
6	3.46167689	-2.41454183	5.08362121

1	3.64248372	-2.73996073	6.11090458
6	4.50763203	-2.49070792	4.13939598
1	5.48208952	-2.87589194	4.44917379
6	4.31471469	-2.08117092	2.81409168
1	5.11627383	-2.13697387	2.07582044
6	3.05271376	-1.59444616	2.45394206
6	2.51469565	-1.09325959	1.19411421
6	2.73940247	-0.55816433	-1.06738864
6	3.52043433	-0.48433333	-2.29681302
6	4.84331157	-0.82976067	-2.59664352
1	5.49494961	-1.24187109	-1.82451975
6	5.29146038	-0.63784866	-3.90967550
1	6.31769759	-0.90360865	-4.17447884
6	4.43552068	-0.11082430	-4.90045991
1	4.81197484	0.02343229	-5.91740371
6	3.11211269	0.23613801	-4.60057290
1	2.44042657	0.63890007	-5.36035564
6	2.66343454	0.04331486	-3.28880176
6	-0.53506403	-1.85153203	-0.52728084
6	3.50525022	-4.77167060	-2.02544948
1	3.55689923	-4.17898917	-1.09807257
1	4.24328381	-4.37630969	-2.73603374
1	3.75212063	-5.81113008	-1.76255596
6	2.08269069	-4.70642565	-2.56176954
6	1.83302836	-3.96041138	-3.73676855
1	2.67637511	-3.45641653	-4.20744210
6	0.55074369	-3.76741921	-4.30100064
6	0.41880839	-2.87862221	-5.52910647
1	-0.22717483	-3.37039000	-6.27162424
1	1.39006241	-2.63128005	-5.97797499
1	-0.07958048	-1.94219247	-5.23123040
6	-2.10548090	-7.30307234	1.56184832
1	-1.43141197	-8.16799654	1.46895157
1	-3.07614306	-7.63163171	1.95803048
1	-1.63965654	-6.60742354	2.27686734
6	-2.22338545	-6.60772067	0.21026556
6	-3.51280522	-6.35990950	-0.31728526
1	-4.37445636	-6.67609138	0.27022479
6	-3.75366286	-5.68744662	-1.53866619
6	-5.19565979	-5.44559438	-1.97039371
1	-5.37868312	-4.36024563	-1.99671505
1	-5.92615899	-5.91873525	-1.29986895
1	-5.33674492	-5.82052029	-2.99539711
7	0.32233316	0.77025923	-3.28917247
7	-1.19431594	0.73587976	-1.38270678
7	-3.23402027	1.02311705	-0.08161187
7	-1.46480787	0.09016852	1.30966396
6	1.37661107	0.28096562	-2.64491690
6	-0.85053339	0.97937558	-2.70089050
6	-2.00813564	1.52193585	-3.40334904
6	-2.20171738	1.93117507	-4.72785176
1	-1.38652005	1.86683557	-5.45033768

6	-3.46473868	2.41774304	-5.08757443
1	-3.64551760	2.74345352	-6.11477136
6	-4.51066959	2.49381080	-4.14331288
1	-5.48510008	2.87915324	-4.45298774
6	-4.31774565	2.08395144	-2.81811197
1	-5.11923001	2.13962175	-2.07974356
6	-3.05577358	1.59703882	-2.45813875
6	-2.51784540	1.09557160	-1.19837270
6	-2.74263516	0.56031362	1.06307048
6	-3.52377182	0.48617150	2.29240685
6	-4.84663940	0.83162537	2.59224808
1	-5.49819873	1.24404738	1.82022488
6	-5.29489665	0.63933762	3.90518905
1	-6.32113215	0.90509947	4.16999956
6	-4.43908293	0.11193063	4.89587622
1	-4.81564811	-0.02263444	5.91273769
6	-3.11566846	-0.23500713	4.59599387
1	-2.44400241	-0.63789112	5.35572685
6	-2.66686958	-0.04175258	3.28432656
25	0.84314805	4.79681664	1.83760005
8	-1.19418322	5.32873168	1.88419289
8	0.53764374	4.25176478	3.84955058
8	2.86117918	5.23367588	2.33069330
8	1.13057489	6.28883531	0.35393963
7	0.79958927	2.94428254	0.87467453
6	0.53222615	1.85349888	0.52331576
6	-3.50230800	4.78105747	2.02856925
1	-3.55496539	4.19254564	1.09859903
1	-4.24157490	4.38443907	2.73717502
1	-3.74668118	5.82221585	1.77004957
6	-2.08009099	4.71012839	2.56511321
6	-1.83279246	3.95878963	3.73717722
1	-2.67758616	3.45516879	4.20566175
6	-0.55092955	3.75911379	4.30016858
6	-0.42135019	2.86325547	5.52334512
1	0.23385142	3.34463190	6.26452800
1	-1.39266281	2.62354768	5.97625623
1	0.06533529	1.92297792	5.21796740
6	2.11448766	7.31261030	-1.54816576
1	1.44191526	8.17828869	-1.45159800
1	3.08592150	7.64125057	-1.94238666
1	1.64777894	6.62108125	-2.26659959
6	2.23050692	6.61089707	-0.19968316
6	3.51927914	6.35785920	0.32698479
1	4.38174502	6.67456627	-0.25904463
6	3.75840323	5.67977666	1.54559148
6	5.19974588	5.43286277	1.97659283
1	5.37984141	4.34696812	2.00006519
1	5.93146043	5.90586303	1.30729768
1	5.34189675	5.80471159	3.00257843

$\{Cryptand(K^+)\}_2\{Mn^{II}(CN)_2Pc(Mn^{II}(acac)_2)_2\}^{2-}$, $S = 11/2$

25	-0.01943859	0.00241732	0.01601042
25	0.13390624	-4.90629744	-1.73470354
8	2.12071869	-5.42248551	-1.40356209
8	0.82773070	-4.16970445	-3.62120974
8	-1.54045152	-5.75095688	-2.72806114
8	-0.45230940	-6.15430969	-0.12045716
7	-2.07900532	-0.60874150	2.63834750
7	0.21923568	-0.70425649	1.83590918
7	2.61094957	-1.16695087	1.80852696
7	1.91003150	-0.19751410	-0.31414399
7	-0.28111696	-2.99678025	-0.96502906
6	-2.60279941	-0.10704405	1.52581907
6	-0.78744421	-0.88998322	2.76763178
6	-0.21904782	-1.48556401	3.97208100
6	-0.78920308	-1.87987492	5.18853913
1	-1.85416978	-1.73323279	5.37418831
6	0.04475277	-2.47476571	6.14319425
1	-0.37308139	-2.79992412	7.09804396
6	1.41626283	-2.68094978	5.88172787
1	2.03362095	-3.17662562	6.63489387
6	1.98749747	-2.28085861	4.66685201
1	3.04175752	-2.45499632	4.44366914
6	1.15862348	-1.66976920	3.71908524
6	1.40875022	-1.16136600	2.37544901
6	2.83073997	-0.72496909	0.57404560
6	4.14558428	-0.74662158	-0.05749027
6	5.40053879	-1.18142403	0.38668002
1	5.51933599	-1.59757475	1.38868183
6	6.48349536	-1.07215974	-0.49539777
1	7.47239943	-1.41744468	-0.18425683
6	6.31656006	-0.53835403	-1.79124235
1	7.17868443	-0.47179941	-2.45797586
6	5.06114424	-0.10706052	-2.23712770
1	4.92025702	0.29701588	-3.24055029
6	3.97777496	-0.21926417	-1.35784267
6	-0.23868938	-1.87345430	-0.61621447
6	4.45763709	-5.08846700	-1.17086906
1	4.37026664	-4.66558440	-0.15805631
1	5.31807830	-4.63578431	-1.67995519
1	4.62454902	-6.16990829	-1.05440597
6	3.14972307	-4.85938572	-1.91071961
6	3.15344465	-4.05173359	-3.07006365
1	4.10345152	-3.61685018	-3.37741219
6	2.01074531	-3.74238088	-3.84353458
6	2.17407573	-2.80377676	-5.03026498
1	1.64194643	-3.21348037	-5.90151748
1	3.22639314	-2.62809824	-5.28858458
1	1.71193369	-1.83438384	-4.78219657
6	-1.76193392	-7.36350820	1.44526256
1	-0.91991394	-8.02702625	1.69237777

1	-2.70426437	-7.92005181	1.53107219
1	-1.75256774	-6.54693911	2.18310586
6	-1.54410756	-6.77685146	0.05839772
6	-2.55096893	-6.96149368	-0.92538689
1	-3.42973699	-7.54204497	-0.64685110
6	-2.48774020	-6.45837511	-2.24111956
6	-3.63959095	-6.75830499	-3.19358054
1	-4.10864125	-5.80942412	-3.50018252
1	-4.39941067	-7.41215185	-2.74469187
1	-3.24015304	-7.23289706	-4.10267710
7	2.04050954	0.61606893	-2.60610995
7	-0.25785283	0.71105412	-1.80356246
7	-2.65024878	1.16965032	-1.77783598
7	-1.94897730	0.20071876	0.34505558
6	2.56328997	0.10907501	-1.49540809
6	0.74942824	0.90072627	-2.73383838
6	0.18264149	1.50422880	-3.93497077
6	0.75447248	1.90581577	-5.14831173
1	1.81964010	1.75990081	-5.33343096
6	-0.07789178	2.50753929	-6.10004730
1	0.34140305	2.83910603	-7.05205176
6	-1.44979181	2.71210013	-5.83915989
1	-2.06610724	3.21311461	-6.58964534
6	-2.02303784	2.30336616	-4.62806309
1	-3.07791766	2.47540087	-4.40621140
6	-1.19536831	1.68698223	-3.68260502
6	-1.44710141	1.16980479	-2.34266151
6	-2.87054143	0.72376356	-0.54494355
6	-4.18733231	0.73584549	0.08274506
6	-5.44446616	1.15880977	-0.36646636
1	-5.56402963	1.57084898	-1.37013615
6	-6.52951314	1.04131606	0.51211555
1	-7.52064466	1.37548705	0.19613474
6	-6.36179785	0.51263969	1.80991315
1	-7.22537628	0.43999180	2.47410634
6	-5.10406696	0.09350654	2.26087182
1	-4.96297222	-0.30705254	3.26565437
6	-4.01907662	0.21216870	1.38446858
25	-0.16159367	4.90766625	1.78008651
8	-2.15638915	5.41310451	1.47932622
8	-0.81736260	4.18826427	3.68624832
8	1.53385788	5.75621480	2.73774640
8	0.39338830	6.15017242	0.15230860
7	0.24244102	2.99711730	1.00955444
6	0.19908266	1.87605097	0.65371197
6	-4.49548318	5.06537635	1.29205141
1	-4.42469711	4.62787818	0.28415607
1	-5.34482914	4.61695116	1.82302746
1	-4.66868350	6.14434886	1.16266991
6	-3.17364256	4.85170557	2.01131005
6	-3.15289115	4.05819773	3.18039118
1	-4.09553657	3.62416832	3.51073086

6	-1.99517165	3.76166481	3.93610574
6	-2.13390494	2.83972133	5.13912964
1	-1.58708814	3.26440502	5.99394199
1	-3.18064933	2.66486476	5.41958945
1	-1.67272069	1.86830930	4.89727985
6	1.66153299	7.36910239	-1.43909480
1	0.81213689	8.03059241	-1.66561974
1	2.59996227	7.92861852	-1.54588323
1	1.63727993	6.55345813	-2.17756853
6	1.47711835	6.78026723	-0.04830235
6	2.50236952	6.97087069	0.91488839
1	3.37236636	7.55585652	0.61867818
6	2.46788055	6.46760631	2.23180493
6	3.63680999	6.77406879	3.16107181
1	4.11508652	5.82792905	3.46177164
1	4.38546501	7.42951932	2.69609100
1	3.25301895	7.24980878	4.07631828
19	-5.68861991	-1.95721436	-5.13538676
8	-4.51940102	-3.08703310	-2.84522151
8	-2.90126920	-1.93777465	-4.99455578
8	-7.82493664	-3.99689934	-5.50213474
8	-5.91550381	-3.49035650	-7.63848789
8	-7.42430948	-0.01082846	-3.88273966
8	-6.12951707	0.66080374	-6.39964650
7	-7.49893164	-2.80048969	-2.75130242
7	-4.02831892	-1.13854368	-7.62997142
6	-6.64280294	-3.54462199	-1.80207099
1	-6.52937108	-4.57390459	-2.17221761
1	-7.12646677	-3.61509405	-0.80336256
6	-5.24261686	-2.96906721	-1.62006309
1	-5.26999442	-1.91164343	-1.29365792
1	-4.73303550	-3.54125259	-0.82145129
6	-3.16074711	-2.61693682	-2.69347258
1	-2.65592548	-3.17456411	-1.88882623
1	-3.17100628	-1.54566457	-2.42230428
6	-2.38841915	-2.82315939	-3.97516775
1	-1.32375365	-2.60825609	-3.78068745
1	-2.45852472	-3.87330704	-4.30840413
6	-2.13251121	-2.00425890	-6.19012722
1	-2.17693538	-3.02722253	-6.61632129
1	-1.06856487	-1.79160166	-5.97419694
6	-2.63440918	-0.94790177	-7.16985158
1	-2.56584785	0.02298469	-6.65964278
1	-1.93443527	-0.90676952	-8.03325860
6	-8.59874208	-3.64645122	-3.23640525
1	-9.36753996	-3.00240782	-3.68869600
1	-9.09164538	-4.19401346	-2.40126860
6	-8.19072125	-4.67001611	-4.29217598
1	-7.34996828	-5.30100638	-3.94707983
1	-9.05245982	-5.33940785	-4.48324522
6	-7.51406924	-4.91853843	-6.54743882
1	-8.38581188	-5.56944552	-6.75686799

1	-6.66321319	-5.56320668	-6.25392758
6	-7.16435918	-4.15738914	-7.81195659
1	-7.10128198	-4.87851730	-8.65063532
1	-7.96441977	-3.42684231	-8.04318057
6	-5.50036032	-2.80696809	-8.82446067
1	-6.24288656	-2.02799500	-9.08605226
1	-5.45696859	-3.51988227	-9.67125589
6	-4.10607832	-2.22084873	-8.62160393
1	-3.45332182	-3.04069380	-8.28882413
1	-3.72572996	-1.89345598	-9.61621262
6	-8.00983102	-1.56803022	-2.12722422
1	-7.19708322	-1.11143635	-1.54477944
1	-8.83156104	-1.78760815	-1.40857030
6	-8.51482424	-0.51189484	-3.10598523
1	-9.30237715	-0.90694553	-3.77809220
1	-8.96587924	0.31144364	-2.51830217
6	-7.80615769	1.08048342	-4.71912416
1	-8.24127062	1.89638423	-4.10971014
1	-8.56580211	0.75512225	-5.45717251
6	-6.58365218	1.61771001	-5.43880402
1	-6.85782248	2.56444384	-5.94435741
1	-5.78569155	1.83483692	-4.70377087
6	-4.98178801	1.13707562	-7.11577080
1	-4.15718589	1.34122500	-6.40931303
1	-5.23065548	2.08842295	-7.62589690
6	-4.57333229	0.11589711	-8.17295761
1	-5.46959971	-0.11501773	-8.76805581
1	-3.84944255	0.60710334	-8.86140449
19	5.71955263	1.95810370	5.10058346
8	4.50127212	3.09656793	2.84109302
8	2.92871096	1.95717184	5.02975562
8	7.88229630	3.97612733	5.41781434
8	6.02614588	3.47468889	7.60170486
8	7.39925414	0.00071530	3.79815419
8	6.16072538	-0.67586779	6.34319051
7	7.47532428	2.79229213	2.67337936
7	4.11424328	1.14172273	7.63543175
6	6.60150554	3.54598342	1.74823671
1	6.50438131	4.57454729	2.12502783
1	7.06102114	3.61691461	0.73820468
6	5.19340469	2.98055838	1.59783527
1	5.20604180	1.92467533	1.26571036
1	4.66790641	3.56001250	0.81497121
6	3.13830674	2.63008391	2.72235342
1	2.61625717	3.18561601	1.92739026
1	3.13887430	1.55758261	2.45554280
6	2.39663129	2.84349255	4.02078905
1	1.32658625	2.63381556	3.85157630
1	2.48046149	3.89396417	4.34976821
6	2.19341844	2.03362671	6.24537414
1	2.26308213	3.05550548	6.67091335
1	1.12129402	1.83519498	6.05806624

6	2.70689037	0.96976874	7.21099856
1	2.61406718	0.00067357	6.70115863
1	2.02838230	0.93526011	8.09165286
6	8.59452005	3.62729484	3.13203196
1	9.36939812	2.97514915	3.56182379
1	9.07014878	4.17346823	2.28601641
6	8.22369401	4.65075269	4.20158152
1	7.38071709	5.29136004	3.88032227
1	9.09689020	5.31052811	4.37315766
6	7.60631048	4.89554438	6.47456537
1	8.48817957	5.53898948	6.66368510
1	6.75300335	5.54802066	6.20643341
6	7.28444840	4.13144733	7.74474451
1	7.24917143	4.84910593	8.58792406
1	8.08477329	3.39377895	7.95097151
6	5.63839655	2.78698742	8.79446521
1	6.37879311	1.99721522	9.02804796
1	5.62929424	3.49387068	9.64737657
6	4.23189584	2.21864920	8.62925380
1	3.57943075	3.04741454	8.31876738
1	3.87682641	1.89023910	9.63277000
6	7.95994774	1.55700402	2.03399191
1	7.12996705	1.10912736	1.46950454
1	8.76687016	1.77094940	1.29719481
6	8.47687364	0.49338536	2.99821279
1	9.28352446	0.87832914	3.65335732
1	8.90589496	-0.33266576	2.39798971
6	7.78648652	-1.10282550	4.61565443
1	8.19460608	-1.91933486	3.98857771
1	8.56905612	-0.79474123	5.33697905
6	6.57518601	-1.62941330	5.36154081
1	6.84768315	-2.58624238	5.84858989
1	5.75531081	-1.82712468	4.64528700
6	5.02684749	-1.14268249	7.08648429
1	4.18159888	-1.33429263	6.40109284
1	5.27769211	-2.09932039	7.58564542
6	4.65815883	-0.12181341	8.15841025
1	5.57220675	0.09561733	8.73114377
1	3.94663270	-0.60743296	8.86345277